COMMENTS ON GAS-FLUIDIZED MAGNETIZABLE BEDS IN A MAGNETIC FIELD
Part 3: Heat Transfer – a reevaluation of the data

by

Jordan Y. Hristov

Review paper
UDC: 537.63:533.6.011.6–912
BIBLID: 0354–9836, *4* (2000), 1, 5–49

In the last two decades a considerable number of communications have been appeared in the field of magnetic stabilization of gas-fluidized ferromagnetic particles. In contrast to the hydrodynamic problems, to the heat transfer problems (temperature distribution in both the axial and radial directions as well as gas-to-particles and bed-to immersed surface heat transfer) have been paid little attention. The present communication made an attempt to re-examine the data concerning the heat transfer phenomena in gas-fluidized beds of ferromagnetic particles controlled by external magnetic field.

INTRODUCTION

Paper idea

The last part of the series considers the heat transfer phenomena in magnetically controlled gas-fluidized beds. The analysis of the data available in the literature will be done on the basis of the hydrodynamic results commented at large in the two previous papers [1, 2].

It is well known that [3, 4] the hydrodynamics conditions (the particle motions and the bubble formation) affect significantly gas-to-particle and bed-to-surface heat transfer as well as the temperature distributions across the bed.

It was well-demonstrated [1, 2] that the external magnetic field allows easy control of the particle mobility by:

- Particle immobilization in MSB (Magn. FIRST) or a Frozen bed (Magn. LAST).
- Reduced particle mobility due to particle aggregation in a fluidized state in spite the magnetization mode [2].
- Reduced bubble formation and appearance [2].

The discussion developed here tends to clarify the results from a position allowing clear identification of the magnetic field effects on the heat transfer. The particle

size effects and the magnetic field control of the particle mobility can be easy related to the well-established facts in the non-magnetic fluidized bed heat transfer [3, 4].

A principle approach in data interpretations and main problems discussed

The present paper re-examines the results available in various literature sources. Most of the data interpretations do not follows those in the paper published. Moreover, in some cases the experimental conditions are re-constructed in order to arrange an almost complete picture of hydrodynamic conditions related to the heat transfer results. All the knowledge available on the fluidized bed hydrodynamics (with and without magnetic fields) was applied for these reconstructions and regime identifications. Despite the non-conventional approach, the paper permits easy comparison of the results on:

- Magnetization modes and magnetic fields applied.
- Particulate materials employed in the studies.
- Overall thermal bed behaviour in different regimes including both the axial and the radial temperature distribution and the effective thermal conductivity.
- Immersed surface-to-fluidized bed heat transfer.
- Data correlations.

EXPERIMENTAL CONDITIONS REVISITING

Magnetization modes applied – a systematization

The knowledge on the hydrodynamics of magnetically controlled gas-fluidized beds indicates that the system would exhibit different regimes with different bed thermal properties. The modes considering the field action require a special attention due to their important effects on the heat transfer phenomena.

The magnetization FIRST and the Magnetization LAST modes have been successfully applied for heat transfer experiments. They have been discussed at large in [1, 2]. Especially for the purposes of the heat transfer Kamholtz [5] (1979) and Levenspiel and Kamholtz [5] (1980) have invented a third magnetization mode. The idea is shown schematically on Fig. 1a. The external magnetic field is applied as pulses termed "field-on" and "field-off" periods respectively. The principle goal of the inventors is to permit a short time (OFF-period) for a particle mixing in the bed that leads to a significant decrease of the axial temperature gradient.

The deep analysis of the experiments carried out by different research group gave a surpassing result. The investigators in the Luikov Inst. of Heat Mass Transfer (Minsk, Belarus) have used the pulsed field magnetization at large for bed-to-surface heat transfer experiments [6–10] too. Zabrodsky and Tambovtsev [7] have been conceived the technique 4 years earlier in 1976.

In fact, the investigators in Minsk [6–10] did not use the terminology of Kamholtz and Levenspiel, but termed the technique as "a magnetization by a pulsed magnetic field". The analysis of their results demonstrates that the ON-OFF field magnetization (a term introduced here) has a modification that follows from the possibility to use an alternating current with an industrial frequency. Figure 1b shows that ON-OFF magnetization may be created if a half of the alternating current is eliminated (by a diode for example). In this case the lengths of both periods are equal.

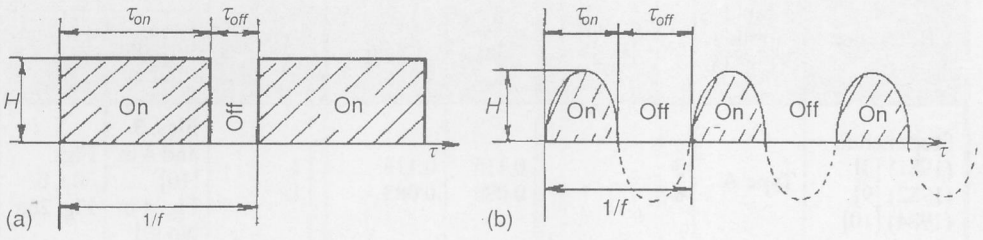

Figure 1. Field ON – Field OFF (ON-OFF) magnetization mode. Schematic descriptions of the magnetic field pulses employed in various studies. First time published graphical interpretations (Present author viewpoint).

(a) Rectangular pulses in accordance with the mode definition invented by Kamholtz [5] and Levenspiel and Kamholtz [6];

(b) ON-OFF mode created by a pulsed sinusoidal field employed in [7–10]

Table 1 summarizes literature data on ON-OFF mode. The data were collected in order to compare the conditions employed by different research groups. The duration of the ON and the OFF periods, and the frequency of the field pulses were calculated (for the first time here) on the basis of various non-systematized data sources (see the last columns of Table 1).

The arrangement of these results in accordance with a third magnetization mode that is neither Magn. FIRST nor Magn. LAST allows a better understanding of the transport process from unified point of view. The recent review of Saxena *et al.* [11] does not consider the pulsed field magnetization in such manner. The advantages and disadvantages of all the three magnetization modes will be discussed further in this paper.

Magnetic fields applied

Table 2 summarizes some details available in the literature in order to clarify this side of the studies performed. The application of axially oriented magnetic fields (generated by solenoids or short coils) dominates [5, 6, 8–10, 12–20]. The only study of Bologa and Syutkin [12] contains a brief remark on the transverse field effect on the heat

transfer. It should be noted that in the dominating situations the problems of the field homogeneity and the field orientation have not been considered (except the woks of Saxena and co-workers [17–20]).

Table 1. Summarized literature data on ON-OFF magnetization mode. The present author did the calculations. In all the cases magnetic fields with axial orientations have been applied.

Reference	Field applied (Fig. 1)	Frequency f, [Hz]	τ_{on} [s]	τ_{off}, [s]	τ_{off}/τ_{on}	Data source	
						Origina lpaper	Present work
Stepanchuk (1981) [8] (1982) [9] (1984) [10]	Type A	3 6	0.116 0.083	0.116 0.083	1 1	Figs. 3 and 4 in [10] Fig. 4 in No [9]	Figs. 30a, b Fig. 26a
Stepanchuk (1982) [9]	Tupe B	50	0.01	0.01	1	Fig. 1–2 in [9]	Fig. 24 Fig. 25a
Stepanchuk (1984) [10]	Type A	2 4 6 8 10	0.01 0.01 0.01 0.01 0.01	0.49 0.24 0.156 0.115 0,09	49 24 15.6 11.5 9	Fig. 4 in [10]	Fig. 30a
Stepanchuk (1984) [10]	Type A	10 10 10	0.01 0.02 0.03	0.09 0.08 0.7	9 8 7	Fig. 4 in [10]	Fig. 30a
Stepanchuk (1982) [10] 4	Type A	$f_{min} = 1$ $f_{max} = 15$	0.01 0.01	0.99 0.056	99 5.66	Fig. 3 in [10]	Fig. 30b
Zabrodsky & Tambovtsev (1976) [7]	Type A	2 5 7 10–15 6–20 25 33	0.01	0.49 0.19 0.132 0.09–0.056 0.0156–0.04 0.03 0.0203	9–5.6 15.66–4 1 1	Fig. 3 in [7]	Fig. 22
	Type B	40 50	0.012 0.01	0.012 0.01	1 1	Fig. 4 in [7]	Fig. 25b
Kambholtz (1979) [5] Levenspiel & Kambholtz (1981) [6]	Type A	0.031	30	2	0.066	Example 1 Table 2	Fig. 6

Table 2. Magnetic fields applied – some details

Reference	*Dc* [mm]	Magnetic system	Mode	Field
Arnaldos [13] Arnaldos *et al*, [14, 15]	70	Solenoid *Ds* = 120 *Ls* = 245 mm	FIRST LAST	Axial (DC) H_{max} = 4 kA/m
Zabrodsky & Tambovstev [7]	92	Solenoid (undefined construction) Some tentative details are available in [18] (*Ds* = 180 mm; *Ls* = unknown)	LAST ON-OFF	Axial, H_{max} = 40 kA/m (AC) (industrial frequency 50 Hz) Axial H_{max} = 40 kA/m (see Table 1)
Bologa & Syutkin [12]	78	Electromagnet (undefined construction)	FIRST	Transverse (AC) (industrial frequency 50 Hz) B_{max} = 16 mT
Bologa & Syutkin [12]	78	Solenoid (undefined construction)	FIRST	Axial (AC) (industrial frequency 50 Hz) B_{max} = 10.9 mT
Neff & Rubinsky [16]	88.9	Solenoid *Ds* ~ 90 *Ls* = 105	FIRST LAST	Axial (DC) B_{max} = 4 mT
Ganzha & Saxena [18]	102	Helmholtz pair	FIRST	Axial (DC)
Qian & Saxena [18]	101.6	Helmholtz pair	FIRST	Axial (DC) H_{max} = 15 kA/m
Dolidovich *et al.* [19]	101.6	Helmholtz pair	FIRST	Axial (DC) H_{max} = 15 kA/m
Saxena & Dewan [20]	101.6	Helmholtz pair	FIRST	Axial (DC) H_{max} = 15 kA/m
Kambholtz (1979) [5] Levenspiel & Kambholtz (1981) [6]	50.8	Undefined magnetic system	ON-OFF	Axial (Pulsed) *H* = 40.317 kA/m (see Table 1)
Stepanchuk [8]	93	Undefined solenoid *Ds* ~ 200 mm *Ls* = 180 mm (tentative)	ON-OFF	Axial, H_{max} = 80 kA/m
Stepanchuk [9]	93	Undefined solenoid	ON-OFF	Axial, H_{max} = 80 kA/m
Stepanchuk [10]	–	Undefined solenoid	FIRST ON-OFF	Axial (AC) (industrial frequency 50 Hz) Axial (Pulsed) (see Table 1)

Gas-solid systems and temperature ranges

Most of the experiments have been performed with iron powders [12], iron shots [12, 16–20], magnetite [7, 10], nickel-kieselguhr catalyst [5, 6], nickel [5, 6, 13–15], ammonia catalyst [21–23] and iron-sand [13–15, 16–20], nickel-sand [13–15] admixtures. In all the cases the fluidizing gas is air except the two cases of exothermic gas reactions in stoichiometric gas admixtures [5, 6, 21–23].

The temperature range does not exceed 100 °C except the two cases of exothermic chemical reactions [5, 6, 21, 22] (see Table 4 below). In all the cases the bed temperature is significantly lower that the particle material Curie point (Table 3). The thermal conditions will be discussed further for each particular case.

Table 3. Currie points of some particulate materials used in the experimetns

Material	Curie point [K]	Data source
Iron	1043	Arnaldos [13]
Nickel	631	Arnaldos [13, 25, 26, 27]
Magnetite	848	Arnaldos [13] Selwood [24]
Ammonia catalyst GK-1 (Russia) as an example	793 (non-reduced)	Vissokov & Ivanov [28]

OVERALL THERMAL BED BEHAVIOUR

Axial temperature distribution

Magnetization FIRST mode

The axial temperature differences along the bed length have been reported non-systematically by several authors. In 1975 Zrunchev [21] has reported that a significant temperature difference across the magnetically stabilized bed exists if the ratio $L/D_c > 6$ (Fig. 2a). Similar curve (Fig. 2b) has been published 10 years latter [22], but for the limiting ratio $L/D_c > 4$. The results of Zrunchev and Popova [23] demonstrate a significant temperature difference across the bed (Fig. 3a). Furthermore, the redrawing of the original figure 3a in a more informative form (Fig. 3b) permits to establish that the results on Fig. 2b and Fig. 3 are similar. On the other hand the lines on Fig. 3b indicate that the field intensity slightly affects the temperature difference across the bed. In all the three cases there is no heating device immersed in the bed (see Table 4).

Table 4. Axial temperature gradients. Stabilization by axial steady magnetic fields. Magnetization First mode (The present author did the calculations)

Reference	Regime	Type of heating	ΔL [mm]	ΔT [K]	$\Delta T/\Delta L$	$\Delta T/\delta_L$ [K]	Data source	
							Original paper	Present work
Zrunchev[21]	MASB Magn. FIRST	Gas preheating at 500 °C and an exothermic chemical reaction of ammonia synthesis	5 *Dc* unknown *Dc*	3.46		0.683	Fig. 2	Fig. 2a lower branch
			5.5 *Dc* unknown *Dc*	68.86		12.52		Fig.2a upper branch
Zrunchev & Popova [23]	MSB Magn. FIRST	Similar conditions	12.45 *Dc* = 0.622 m at $r/r_c = 0$	120	249–256	20–20.6 ! variations with H (see Fig. in the present work)	Fig. 5	Fig. 2b
Zrunchev & Popova [23]	MSB Magn. FIRST	Similar conditions	3. *Dc* unknown *Dc* *at* $r/r_c = 0$	45		13.46 See also Fig. in the present work	Fig. 7.	Fig. 3

Table 4. *Continuation*

Reference	Regime	Type of heating	ΔL [mm]	ΔT [K]	$\Delta T/\Delta L$	$\Delta T/\delta_L$ [K]	Data source	
							Original paper	Present work
Arnaldos [13]	Fixed bed $H = 0$ A/m	Immersed heater (Fig. 4)	1.28 Dc = 0.090 m at $r/r_C = 0.214$	73.69	859.38	60.62	Fig. IV-3	Fig. 5a
	Fluidized bed $H = 0$ A/m	Immersed heater (Fig. 4)	1.28 Dc = 0.090 m at $r/r_C = 0.214$	7.142	80.356	5.67	Fig. IV-6	Fig. 5b
	MSB Magn. FIRST	Immersed heater (Fig. 4)	1.28 Dc = 0.090 m at $r/r_C = 0.214$	64.74 at $H = 2$ kA/m	728.34	51.38	Fig. IV-10	Fig. 5c
				81.42 at H = 4 kA/m	916.05	64.62	Fig. IV-9	Fig. 5d
Kamholtz [5] Levenspiel & Kamholtz [6]	MSB Magn. FIRST $H = 40.317$ kA/m Steady state operation	Gas preheating at 218 °C & an exothermic chemical reaction of methane synthesis	216 Dc = 0.11 m at $r/r_C = 0$ 10 min. operation	60	545.45	27.77	Table II	Fig. 6
			216 Dc = 0.11 m 45 min. operation at $r/r_C = 0$	58	527.27	26.85		

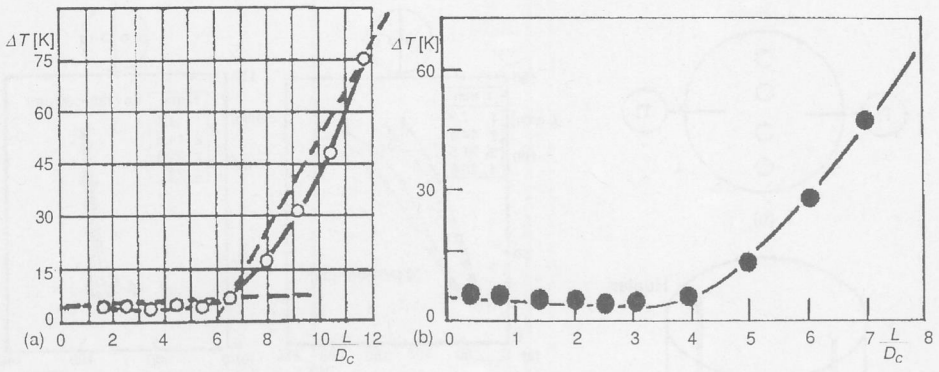

Figure 2. Zrunchev's results on axial temperature difference across the bed. A relationship between ΔT and the dimensionless bed height L/D_c

(a) Results from [21]. Conditions are summarized in Table 4. Pressure of 10 MPa. The present author adds the dashed lines;

(b) Data of Zrunchev and Popova from [22]. Pressure of 30 MPa

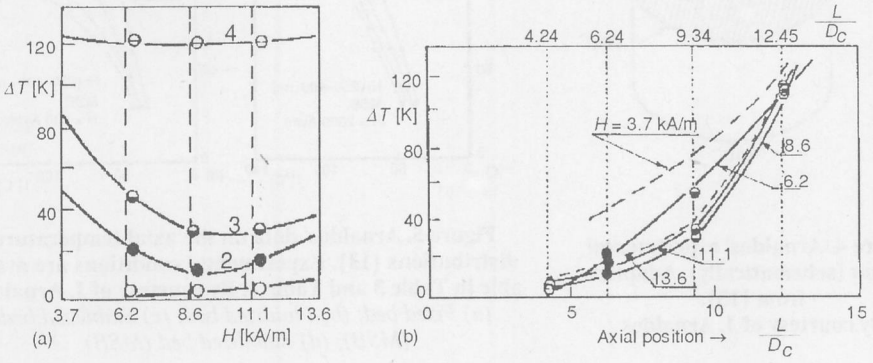

Figure 3. Results of Zrunchev and Popova from [23]. Conditions in Table 4.

(a) Original figure; (b) Data rearrangement by the present authors

In 1986 Arnaldos [13] has reported systematic results on the heat transfer in magnetically controlled bed with an immersed electric heater (Fig. 4). The axial temperature distributions in three regimes are shown on Fig. 5. All the measurements have been performed in a plane oriented normally with respect to the heater plane (See inset). The axial temperature profiles in fixed and the stabilized bed are similar, while those in the fluidized bed are approximately 10 time lower. Kamholtz [5], Levenspiel and Kamholtz [6] as a comparative example concerning ON-OFF magnetization mode (see below the white labels on Fig. 6) have reported similar results.

More valuable information may be obtained if all the data available are recalculated by an unified approach. In order to compare the axial temperature gradients the

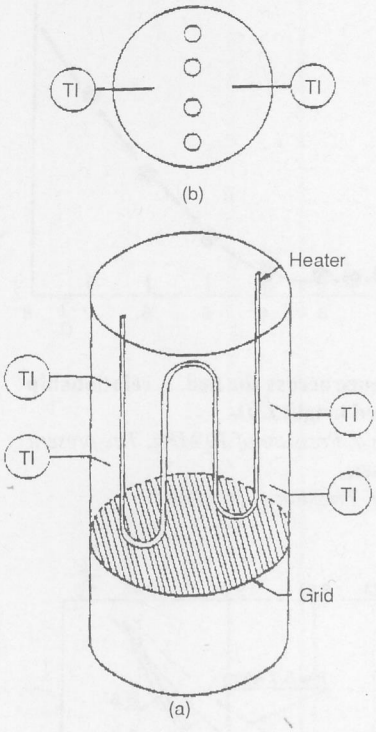

Figure 4. Arnaldos' experimental set-up (schematically). Adapted from [13]. By courtesy of J. Arnaldos

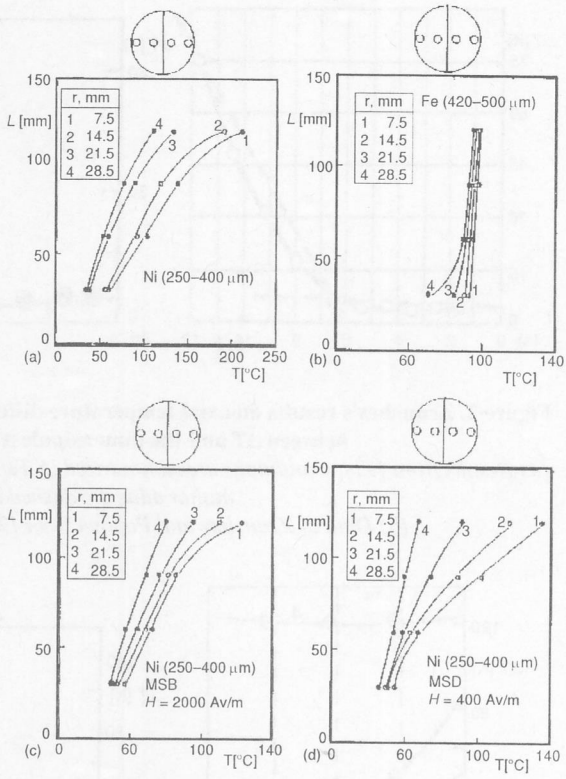

Figure 5. Arnaldos' data on the axial temperature distributions [13]. Experimental conditions are available in Table 3 and Table 4. By courtesy of J. Arnaldos
(a) Fixed bed; (b) Fluidized bed; (c) Stabilized bed (MSB); (d) Stabilized bed (MSB)

results shown on Figs. 2–6 were treated in the present work with a digitizer and were calculated as:

$$\text{grad}T_a = \frac{\Delta T}{\Delta L} \tag{1a}$$

$$\text{or}\,\Delta T_a^* = \frac{\Delta T}{\delta_L} \tag{1b}$$

The second pseudo gradient ΔT_a^* was used in the cases when the bed length was unknown, but it was possible to use the ratio L/D_c (the results of Zrunchev for example).

All the data calculated in accordance with Eq.1a are summarized in Table 4.

ON-OFF magnetization mode

The results of Kamholtz [5] and Levenspiel and Kamholtz [6] are shown on Fig. 6. The data plotted demonstrate the advantages with respect to the Magnetization FIRST mode. The axial temperature gradients are shown in Table 5.

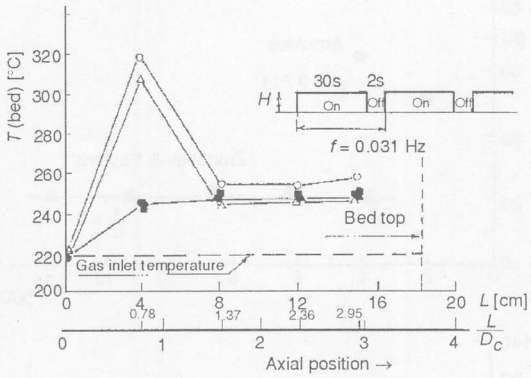

Figure 6. Results of Kamholts [5] and Kamholtz and Levenspiel [6]. A graphical presentation of the data from Table 1 and Table 2 in [5, 6]. Simultaneous presentation of the temperature distribution with the Magnetization FIRST mode (white labels) and the ON-OFF mode (solid labels). Inset, ON-OFF conditions employed

Table 5. Axial temperature gradients. Stabilization by axial magnetic fields with ON-OFF Magnetization mode (The present author did the calculations)

Reference	Regime	Type of heating	ΔL [m]	ΔT [K]	$\Delta T/\Delta L$ [K/m]	Data source	
						Original paper	Present work
Kamholtz [5] Levenspiel & Kamholtz [6]	MSB H = 40.137 kA/m	Gas preheating at 218 °C and methane synthesis	2.16 Dc = = 0.11m 13 min period	2	18.18	Table 1	Fig. 6
			2.16 Dc = = 0.11m 33 min period	1	9.09		
			2.16 Dc = = 0.11m 58 min	5	45.45		

Effects of the field intensity and the radial position of measurements

These effects cannot be evaluated from the data published. However, some non-systematic data collected from accidentally performed experiments are shown in Figs. 7 and 8. Unfortunately, there are no comments of the phenomena in the original

works. Zrunchev [21] has commented that the increased field intensity has led to better temperature distribution across the bed. However, the data plotted on Fig. 3 do not confirm this conclusion. Moreover, the plots on Fig. 7 show that there is no field effect on the axial temperature profile.

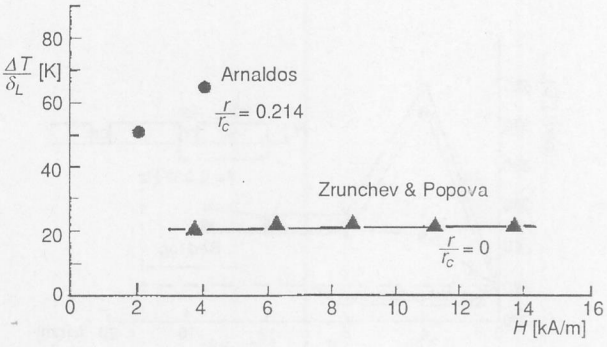

Figure 7. Magnetic field effects on the axial temperature gradients

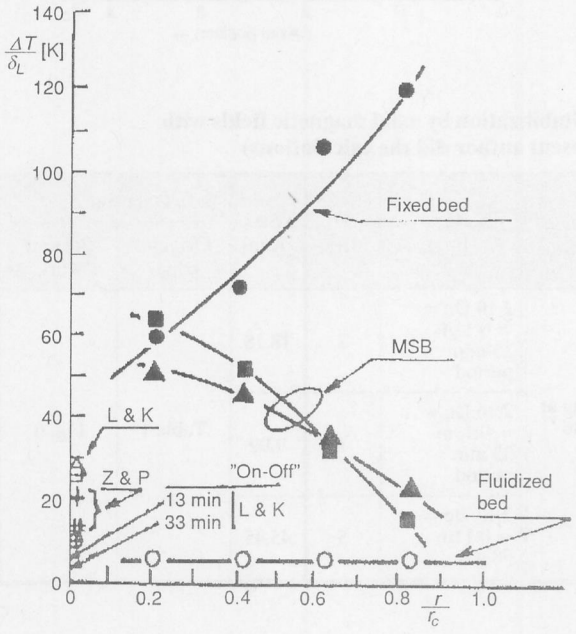

Figure 8. Axial temperature gradients as a function of the radial positions of measurements. Magnetization FIRST mode. A graphical presentation of some results summarized in Table 4 and Table 5

Arnaldos' data – solid labels (●, ■, ▲, ○); *L & K – Levenspiel and Kamholtz [5, 6]* (□, △); *Z & P – Zrunchev and Popova [22, 23]* (+, #); *Zrunchev [21]* (⊕)

The radial position of the measuring points strongly affects the axial temperature gradient. The state of MSB demonstrates that the movement of the measuring point from the bed centreline toward the column wall decreases the axial temperature gradient. Near the wall the values of $\Delta T/\delta_L$ aspire those of the fluidized bed without field effects. This behaviour is just the opposite of that demonstrated by a fixed bed. An explanation of the

differences may be found in the particle arrangement and the velocity profiles (see comments below).

Radial temperature profiles (magnetization FIRST mode)

Arnaldos [13] and Arnaldos *et al.* [14, 15] have measured the radial temperature profiles only. Some valuable data are shown on Fig. 9. The plots (Figs. 9b, c) demonstrate clearly that radial temperature gradients in MSB are lower than those demonstrated by

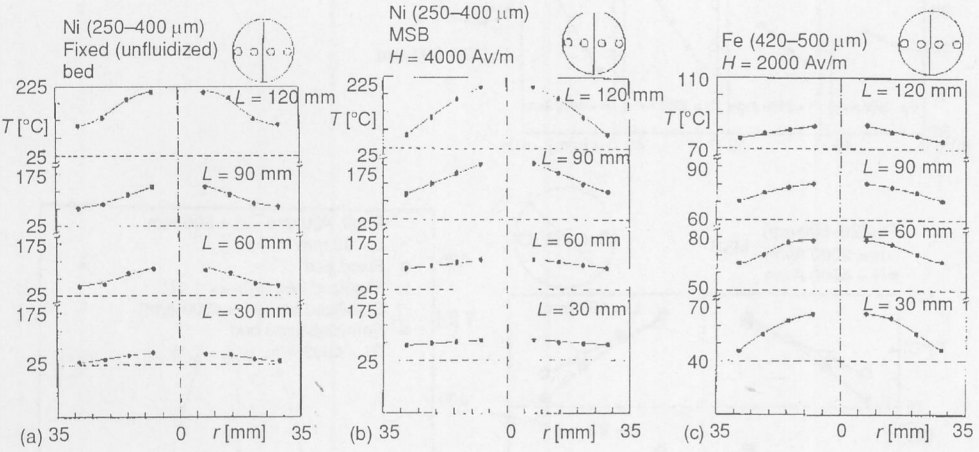

Figure 9. Radial temperature profiles in a direction normal to the heater plane. Results of Arnaldos.

(a) Fixed bed [13]; (b, c) Stabilized beds [13]; By courtesy of J. Arnaldos.

an ordinary fixed bed (Fig. 9a) of the same particulate material. The reason of that originates in the particle arrangement induced by the field lines.

The change of the direction of the measuring plane (see the inset of Fig. 11) affects the slope of the radial temperature profiles (Fig. 11a, b). Similar effect may be found on Fig. 10a, b as a result of the increasing field intensity. Figure 12 summarizes all the data available on the field intensity effect (recalculated as a radial temperature gradient).

The plots of Arnaldos's results (Figs. 9–11) demonstrate a length effect on the radial temperature profile. In order to obtain a more comprehensive information all the data were recalculated as radial temperature gradients. The results are shown on Fig. 13 (key to Fig. 13 is given in Table 6).

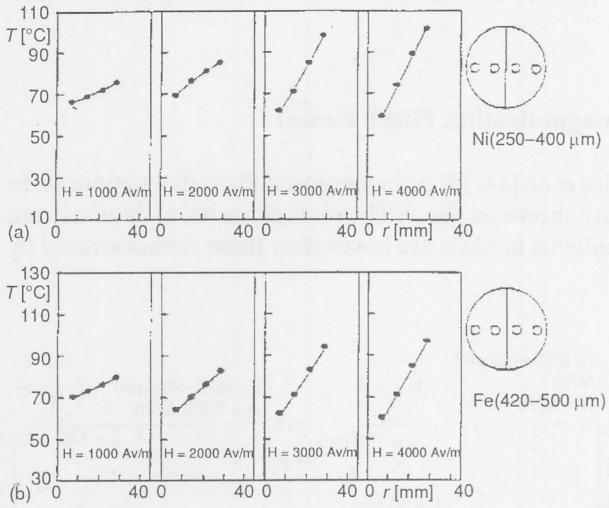

Figure 10. Field effect on the radial temperature profiles [13, 15, 29] Adapted from [13]. By courtesy of J. Arnaldos (see also Fig. 6 in [15] and Fig. 9 in [29])

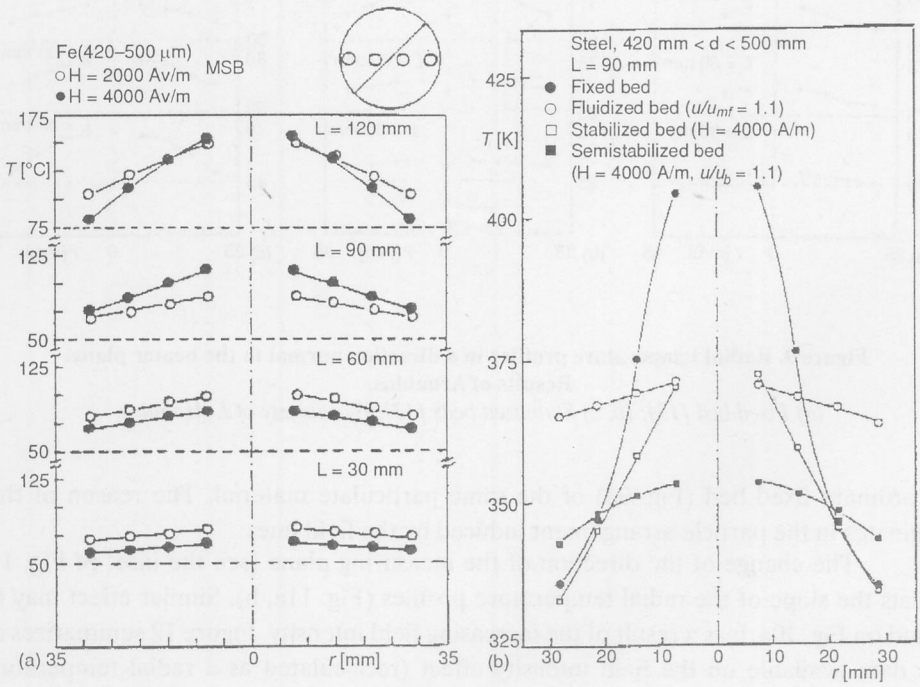

Figure 11. Radial temperature profiles

(a) In the regime of MSB [13] (A superposition of Figs.IV–11 and IV–12 in [13]). Effect of the measuring plane orientation (45° with respect the heater plane); (b) Examples of radial temperature profiles in different bed regimes. Adapted from [13] (see also Fig. 7 in [15] and Fig. 8 in [29]). Measuring plane orientation normal to the heater plane. By courtesy of J. Arnaldos

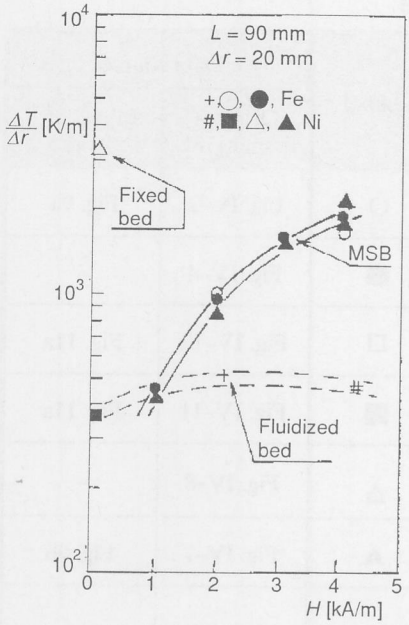

Figure 12. Field intensity effect on the radial temperature gradients. Data obtained by a re-calculation of Arnaldos's results [13] (Original data from Figs. IV 11, 12, 15, 16 in [13]) Present work – Figs. 9, 10, 11a (Note: All the data correspond to $\gamma = 90°$ except ○, $\gamma = 45°$)

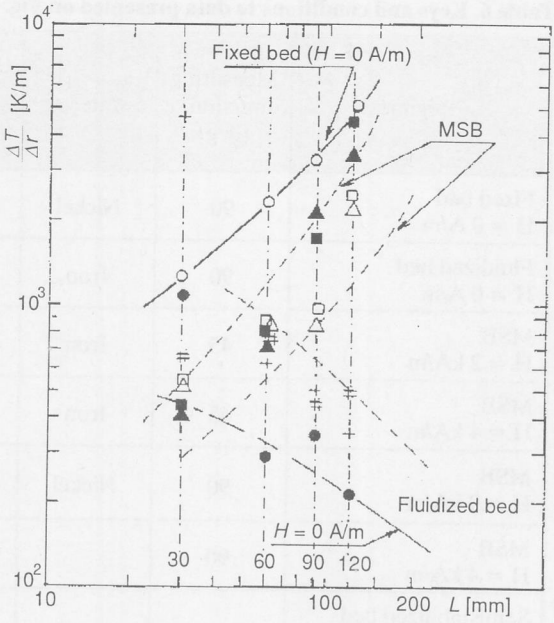

Figure 13. Length effects on the radial temperature gradients. Re-calculation of the data presented in Figs. 9–11

Effective thermal conductivity [13, 15]

The temperature distribution inside the bed and the heat transfer rate are strongly affected by the bed effective thermal conductivity, K_b. The coefficient K_b has been calculated on the basis of a mathematical model in a general form:

$$K_b\left(\frac{\partial^2 T}{\partial x^2}+\frac{\partial^2 T}{\partial y^2}+\frac{\partial^2 T}{\partial z^2}\right)=U\rho C_p\frac{\partial T}{\partial z} \tag{2}$$

The contribution of the vertical conduction has been neglected due to the superimposed effect of the convection. On the other hand, due to geometrical structure and symmetry the equation (2) has been expressed as

Table 6. Keys and conditions to data presented on Fig. 13

Regime	Measuring direction, γ [deg]	Material	Symbol	Data source	
				Original paper [13]	Present work
Fixed bed H = 0 A/m	90	Nickel	○	Fig. IV–2	Fig. 9a
Fluidized bed H = 0 A/m	90	Iron	●	Fig. IV–4	–
MSB H = 2 kA/m	45	Iron	□	Fig. IV–12	Fig. 11a
MSB H = 4 kA/m	45	Iron	■	Fig. IV–11	Fig. 11a
MSB H = 2 kA/m	90	Nickel	△	Fig. IV–8	–
MSB H = 4 kA/m	90		▲	Fig. IV–7	Fig. 9b
Semistabilized bed (Fluidized bed at H = 2 kA/m)	90	Iron	+	Fig. IV–14	–
Semistabilized bed (Fluidized bed at H = 4 kA/m)	90	Nickel	#	Fig. IV–13	–

$$K_b\left(\frac{1}{r}\frac{\partial T}{\partial r}+\frac{\partial^2 T}{\partial r^2}+\frac{1}{r^2}\frac{\partial^2 T}{\partial \theta^2}\right)=U\rho_g C_p\frac{\partial T}{\partial z} \tag{3}$$

It has been assumed that the heating surface (see in Fig. 4) is continuous over the X–Z plane (the heat flux has been assumed perpendicular to that plane, on its two surfaces).

The inlet gas temperature has been assumed as room temperature, therefore

$$T = T_0 \text{ at } z = z_0$$

The boundary conditions for any quadrant of the bed cross-section (Fig. 14a). The heat convection between the bed and the environment has been described as

$$\frac{\partial T}{\partial r}=-\frac{h}{K_b}(T-T_0) \quad \text{at} \quad r=R \tag{4}$$

Further, it has been assumed no heat flux through the vertical plane perpendicular to the heating system (see Fig. 14a):

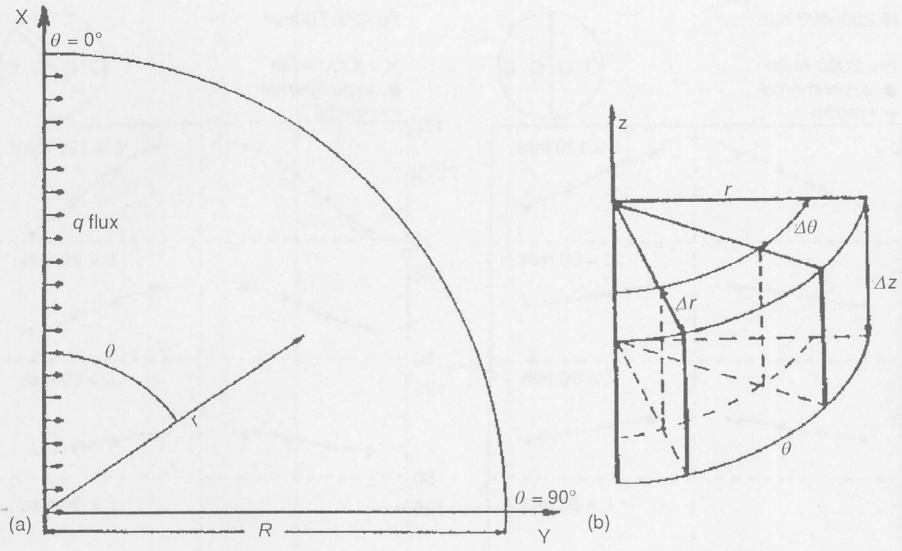

Figure 14. Elements of the model formulation
(a) Definition of the boundary conditions (Fig. IV–9 in [13]) (See also Fig. 9 in [15])
(b) Discretization of the bed (Fig. IV–20 in [13])

$$\frac{\partial T}{\partial \theta} = 0 \quad \text{at} \quad \theta = 90° \tag{5}$$

On the other hand, at $\theta = 0$ the boundary conditions has been written as

$$\frac{\partial T}{\partial \theta} = -\frac{Qr}{SK_b} \tag{6}$$

The last boundary condition has been established for $r = 0$ (under the assumption that there are no variations of T with θ, so

$$\frac{\partial T}{\partial \theta} = -\frac{Q \sin\theta}{SK_b} \quad \text{at} \quad r = 0 \tag{7}$$

The model has been solved numerically by an implicit procedure and a system discretization ($\Delta\theta = 5°, \Delta r = 4.375$ mm, $\Delta z = 0.5$ mm) (Fig. 14b). The temperature profiles obtained by the model are shown in Fig. 15.

To obtain the optimum values of K_b an objective function has been defined in order to obtain minimized differences between the measured and the calculated values of T. The optimization has been achieved through the minimization of the parameter

$$F = \frac{1}{n_i} \sum_{i=1}^{n} \left[\frac{T_{\exp} - T_{cal}}{T_{\exp}} \right]^2 \tag{8}$$

The variations of k_b with H are shown in Fig. 16

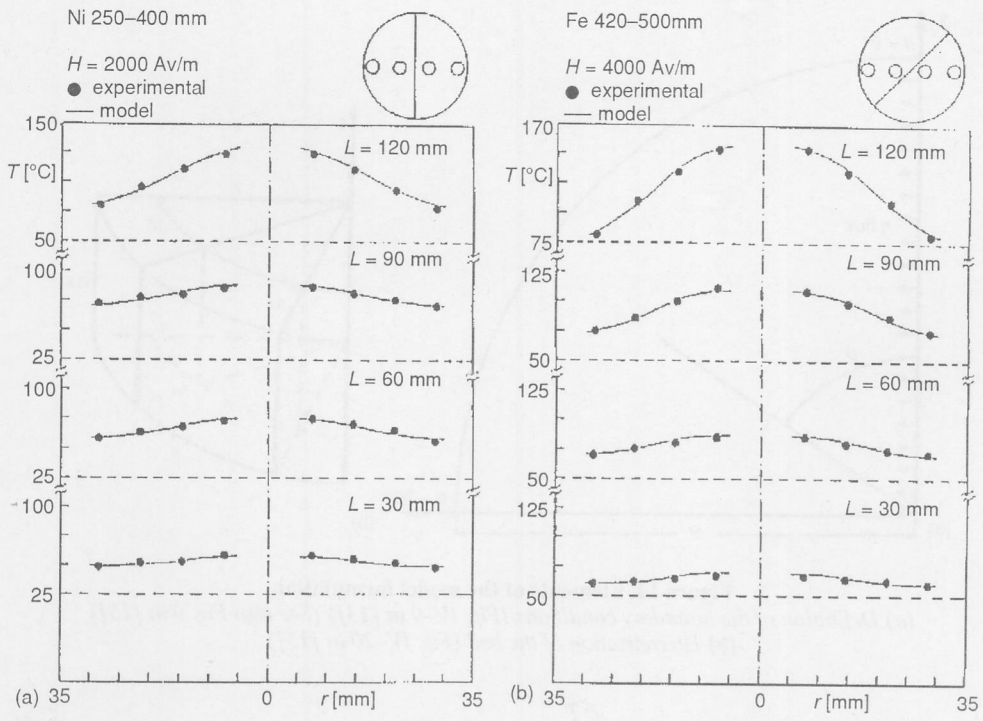

Figure 15. Radial temperature profiles in MSB – a validation of the model [13]
(a) Nickel particle bed (Fig. IV–23 in[13]) (See also Fig. 2 in [15])
(b) Iron particle bed (Fig. IV–24 in [13])

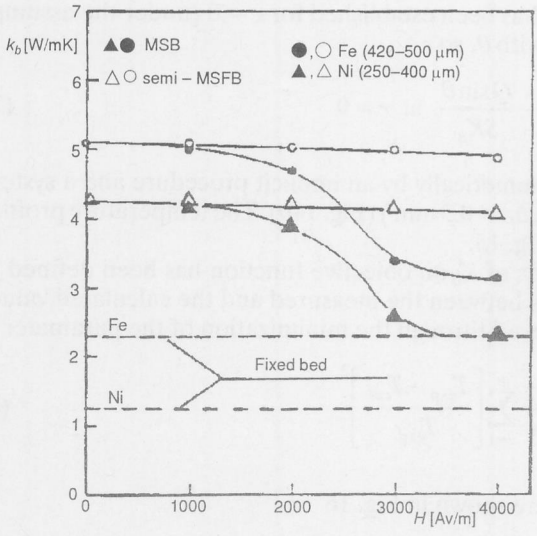

Figure 16. Variations of the effective thermal conductivity with the field intensity [13] (see also Fig. 11 in [15] and Fig. 10 in [29])

Comments on the overall bed thermal behaviour

The data re-examined in the previous points demonstrate several major thermal properties of gas fluidized beds of magnetizable particles that are induced by the magnetic field applied.

(1) Stabilized beds (Magnetization FIRST mode):

- First of all, the stabilized bed demonstrate significant axial temperature gradients (Table 4 and Figs. 3b, 8, 11, 13).
- Second, the axial temperature profiles are strongly affected by the radial position of measurement (Fig. 8).
- Generally the axial temperature gradients decreases toward the column wall (Fig. 8) and approach values demonstrated by the fluidized beds unaffected by any field action.
- Third, the stabilized bed demonstrates a significant field effect on the axial temperature profiles (Figs. 7, 11a, 12).
- Fourth, the radial temperature profiles (Arnaldos' results) and the calculated radial gradients exhibit also field effects (Fig. 12) as well as significant length effects (Fig. 13). (*i. e.* the radial temperature gradients depend on the axial position along the bed axis-see below).

All these properties are similar to those exhibited by the conventional packed bed [30–33]. They support the opinion that the magnetically stabilized is a packed bed without particle motions. All the effects mentioned above may be explained by the particle arrangement along the field lines. I should note again, that all the data commented above have been obtained in axial magnetic field. The simultaneous action of the fluid flow and field forms a packed bed with anisotropic structures [1, 34] situated between two limiting particle arrangements:

(I) an ordinary packed bed with isotropic properties (before the onset of MSB), and
(II) a bed consisting of streamlined aggregates and channels dividing them (just before the breakdown of MSB).

The significant field effect on the radial temperature gradients may be attributed to the decreased lateral thermal conductivity of the bed parallel to the development of the anisotropy of the bed structure. For example, the second limiting particle arrangement may be considered as a bundle of "bars" with significant gas gaps between them. Such system demonstrates significant lateral gradients. This mechanistic interpretation could explain the field effect on the radial temperature distribution. Furthermore, in all the experiments commented a radial adiabaticity has not been created. Thus, the radial heat conduction has not been eliminated like in well-designed special experiments [33].

The axial length effect on the radial temperature profiles (the experiments of Arnaldos) resemble that existing conventionally packed beds (see for example [31, 32]). As commented in [32] most of the data is obtained in a Graetz-type experiments. In a packed bed the entry length effect (Graetz heat transfer problem) much less likely exist [32]. The Arnaldos' results (see the slope of the radial temperature profile at different axial position) indicate that the effective thermal conductivity K_b depends on the length

This conclusion has not been commented by Arnaldos, because his model is more simplified.

On the other hand, if q ($q = K_b \cdot \partial T / \partial r$) is a constant along the bed, the increase of $\partial T/\partial r$ in any directions indicates that K_b decreases that is consistent qualitatively with the results obtained with non-magnetic packed beds [32]. No explanations are available in the literature, but the data on Fig. 16 indicate that Arnaldos's model assumption of the homogeneity of the bed structure is an oversimplification. A model assuming an anisotropy of the thermal conductivity of MSB has not been developed yet.

However, Arnaldos' results (see Fig. 16) show that at zero field intensity the thermal conductivities of the stabilized and the ordinary packed beds are different, but become almost equal under the action of high field intensities. From the point of view of the existing particle arrangements in the bed such behaviour is strange. First of all, it is impossible to create at $H = 0$ simultaneously a fixed bed or MSB (the possible bed regimes are a fixed bed or a fluidized bed [1, 2, 34]). Second, at high intensities the bed may be fixed or stabilized. Third, the model does not concern the gas velocity effect on the particle arrangement in MSB. The comments on the model are not critique (the Arnaldos's contributions in the studies of MSB are significant), but they focus the attention on the fact that the assumption of the bed homogeneity imposed by the concepts of Rosensweig [35–37] (see comments in [1]) does not work.

(2) Fluidized bed (magnetization FIRST mode):

Any particle motions available in the bed due to the fluidizing gas significantly reduce both the axial (Fig. 5b, 8, Table 4) and the radial (Figs. 11b, 12, 13) temperature gradients. The magnetic field effect on fluidized particles (a semi-stabilized bed in accordance with Arnaldos) may be associated to the reduced particle mobility. The reduced contribution of the particle convection leads to greater radial (Fig. 11b, 12, 13) and axial gradients with respect to the case of a non-magnetic fluidized bed [3, 4].

(3) ON-OFF magnetization effects:

The intermittent magnetization with the ON-OFF mode may be considered as an alternative solution avoiding the significant temperature gradients in MSB. The results summarized in Table 5 and those plotted on Figs. 6 and 8 clearly demonstrate that the ON-OFF technique reduces significantly the axial temperature gradients. Moreover, the data of Kamholtz [5] and Kamholtz and Levenspiel [6] (Table 1 and 2 in [5, 6] – not shown here) show that there are no length effect on the axial temperature profiles (see Arnaldos data – Figs. 5 too). Unfortunately, no data are available on the effect of that magnetization mode on the radial profile.

The data re-examined here indicate that much future work should be done for better investigation of the overall temperature behaviour of gas-fluidized magnetically controlled beds. Moreover, the fluidized system offers a wide area of application of various magnetization (or fluidization) modes that may enhance the thermal properties of such beds.

BED-TO-IMMERSED SURFACE HEAT TRANSFER

The heat transfer exchange with an immersed surface is the second important problem considered by many investigators. In order to clarify the contributions and the main results the analysis will be done in accordance with the already defined magnetization modes. It was already discussed at large that the magnetically controlled magnetizable bed exhibit different behaviours as a result of the simultaneous action of both the field and the fluid flow. This reflects directly on the bed thermal characteristics as commented in the previous part of the present work. Now, the heat transfer to an immersed surface is the focus of the commentary.

The re-examination of the data done here has been provoked by the fact that most of the investigators (whose results are discussed in this section) have been focussed the attention on heat transfer results, but not on the hydrodynamic effects on them. Most of the basic results on the heat transfer in magnetically controlled fluidized beds [12, 16] have been obtained without taking into consideration the differences in the bed behaviour in the various regimes. The review of Saxena *et al.* [11] does not give answers of the problems. The reason of the discrepancies in the results is due to different bed hydrodynamics interpretations and the clear identification of the regime available under the simultaneous action of both the gas flow and the external magnetic field.

The successful combination of the already available results on the heat transfer [11–20] and the recent results on bed hydrodynamics [34, 38] (see also comments in [2]) allow a re-examination of the results. The hydrodynamics effects and the experimental conditions on the maximum and the minimum wall-to bed heat transfer coefficients have been discussed in order to clarify the results obtained by various research groups.

Major experiments performed

The experiments carried out by different authors are summarized in Table 7. Some detailed conditions concerning the ON-OFF magnetization mode were already presented in Table 1. The details will be discussed separately.

Particles used and other conditions

The data summarized indicate that there are two different situations studied. The results obtained with pure ferromagnetic particle beds are discussed only. The experiments with admixtures of magnetic and non-magnetic particles [7, 11, 13–15, 17] will not be commented in the present paper. The dominating particle material is the iron [12–20], and in some particular cases nickel [13–15, 29] and magnetite [7, 8, 10] are used. This allows easy comparative calculations in order to establish common tendencies of the results re-examined.

Table 7. Previous studies on heat transfer between immersed surfaces in magnetically controlled beds of pure ferromagnetic particle beds – some details

Solids-Fluid	d_p [μm]	Mode	Field	Probe	Probe Power [W]	T_w [°C]	Reference
Steel- Air Nickel-Air	420–500 250–500	FIRST LAST FIRST	Axial (DC) 4kA/m	Four vertical tube heaters	35; 95; 188	–	Arnaldos *et al.* [13–15, 29]
Iron powder-Air	0–40; 40–60; 60–90	FIRST	Tranverse (AC) B_{max} = = 16 mT	Vertical cylinder	–	–	Bologa & Syutkin [12]
Iron powder - Air	169–200 200–250 250–500	FIRST	Axial (AC) B_{max} = = 10.9 mT	Vertical cylinder	–	40; 60 85	Bologa & Syutkin [12]
Iron shot-Air	727	FIRST LAST	Axial (DC) B_{max} = = 4 mT	Vertical plate	–	60	Neff & Rubinsky [16]
Iron shot-Air	1086	FIRST	Axial (DC)	Horizontal cylinder		50	Ganzha & Saxena [17]
Iron shot-Air	733	FIRST	Axial (DC) H_{max} = = 15 kA/m	Horizontal cylinder		50	Qian & Saxena [18]
Iron shot-Air	733 1511	FIRST	Axial (DC) H_{max} = = 20 kA/m	Horizontal cylinder		50	Dolidovich *et al.* [19]
Iron shot-Air		FIRST	Axial (DC) H_{max} = = 20 kA/m	Horizontal cylinder		50	Saxena & Dewan [20]
Magnetite-Air	300	ON-OFF	Axial (pulsed) See Tables 1 and 2	Vertical plate	–	60	Zabrodsky & Tambovtsev [7]
Magnetite-Air	?!	ON-OFF	Axial See Tables 1 and 2	A steel sphere of 30 mm diameter		70–900*	Stepanchuk [8]
Undefined magnetic particle- Air	300	ON-OFF	Axial see Tables 1 and 2	Vertical plate	–	–	Stepanchuk [9]
Magnetite-Air	?!	ON-OFF	Axial See Table 1 and 2	Undefined	–	–	Stepanchuk [10]

* – Note: The sphere has been heated preliminarily in a furnace and after that immersed into the bed. The nonsteady heat transfer has been studied.
?! – undefined

Heat transfer probes

In all the studies electrically heated probes with a constant heat flux q have been employed. The experiments with vertical surfaces are only two: a vertical plate probe [4, 16] and a vertical cylinder [12]. Multiple tubes heat transfer probe has been applied by Arnaldos *et al.* [13–15, 29]. These probes permit the average heat transfer coefficient, h_w to be determined only. Saxena and co-workers [11, 17–20] have applied a horizontal tube probe described by Brich *et al.* [40] (see also, 11, 17–20]).

Two approaches in surface temperature T_W measurements have been applied. The first approach is to measure directly T_w by thermocouples [16]. The second and more popular approach is to constitute the probe as an arm of a Watson electric bridge [7, 11, 12, 18–20]. This allows easy establishment of a constant probe surface temperature and easy control of the heat flux $\dot{q}$ (Ganzha & Saxena, 1998). The overall heat transfer coefficient is defined by

$$h_w = q\,(T_W - T_b)^{-1} \tag{9}$$

Magnetization modes applied

The magnetization modes and some details are summarized in Tables 1, 2 and 7. The application of axial magnetic field generated by solenoids [7, 12, 13–16] and Helmholtz pairs [18–20] dominates. Bologa and Syutkin [12] have been applied a transverse field only. All these studies have been performed with both classical modes-Magnetization FIRST or LAST.

A special group of investigations are those performed in Minsk Inst. of Heat Mass Transfer. All of them have been carried out in accordance with the ON-OFF mode.

Regimes created

The bed description available in the works discussed here follow two conflicting bed interpretations [1, 33]:

- The earlier studies (Zabrodsky & Tambovtsev) [7], Bologa & Syutkin) [12], Neff & Rubinsky [16]) follow the description consisting with the classical postulations in fluidization. In accordance with these authors the stabilized bed is a transitional state between the initial fixed bed and the fluidization onset. The fluidization starts at its breakdown and the onset of unrestricted particle motions (velocity, U_{mf}) [1, 2, 33].
- The studies of Saxena's group follow the Rosensweig's interpretation [35–37], *i.e.* the onset of MSB at a velocity close to U_{mf0} is assumed as the fluidization onset. The same concept has been accepted by Arnaldos *et al.* [13, 15, 29].

The results published cover the fixed bed, stabilized bed and fluidized bed regimes in accordance with the Magnetization FIRST and LAST modes. The differences in bed descriptions will be taken into consideration during the re-examination of the

results. However, the phenomena analysis and the reconstruction of the experimental situations will follow the first point of view consistent with the classic fluidization results on hydrodynamics [40] and fluidized bed heat transfer [3, 4]. A special attention will be paid on the ON-OFF mode (neither FIRST nor LAST) as a first review on that mode appearing in the literature.

Major results experimental findings

Magnetization FIRST mode

Vertical surfaces

The first results reported by Bologa and Syutkin [12] are shown in Fig. 17. The plots indicate that the heat transfer coefficients in an axial field (Fig. 17a) have maxima.

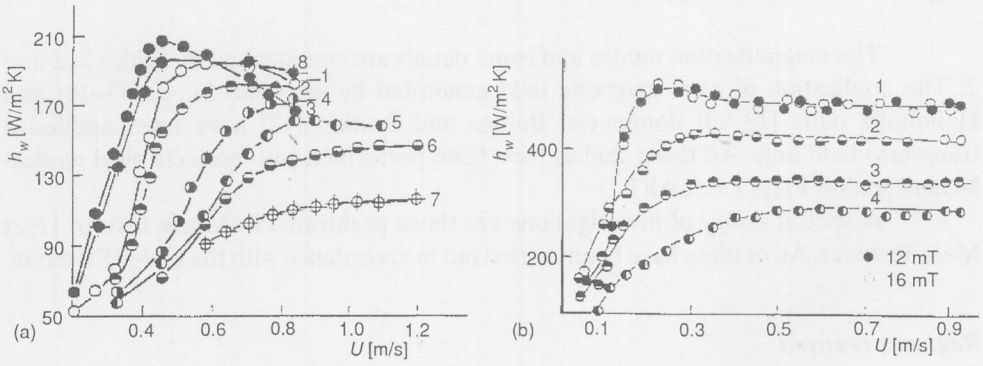

Figure 17. Bologa and Syutkin [12] data (Magn. FIRST)

(a) Axial field. Iron powder, 250–500 μm; h_{b0} = 130 μm; Dc = 78 mm. Effect of the field intensity on the heat transfer coefficient. Magnetic field induction (mT): Lines: 1 – 5; 2 – 6.16; 3 – 0; 4 – 7.46; 5 – 8.6; 6 – 9.25; 7 – 10.9; 8 – 3.25

(b) Transverse field. A simultaneous effect of the field induction and the particle diameter on the heat transfer coefficient. h_{b0} = 320 mm; Dc = 78 mm. Iron powder; Lines: 1 – (0 – 40 μm); 2 – (40 – 60 μm); 3 – (60 – 90 μm); 4 – 90–140 μm); Field induction, B (mT); ● – 12; ○ – 16

In contrast to these results, the plots obtained with a transverse field practically do not exhibit such behaviour. Moreover, the values obtained in a transverse field are twice lower that those in an axial field. Similar results have been reported by Neff and Rubinsky [16] (Fig. 18a), Arnaldos *et. al* [13, 14, 29] (Fig. 19a).

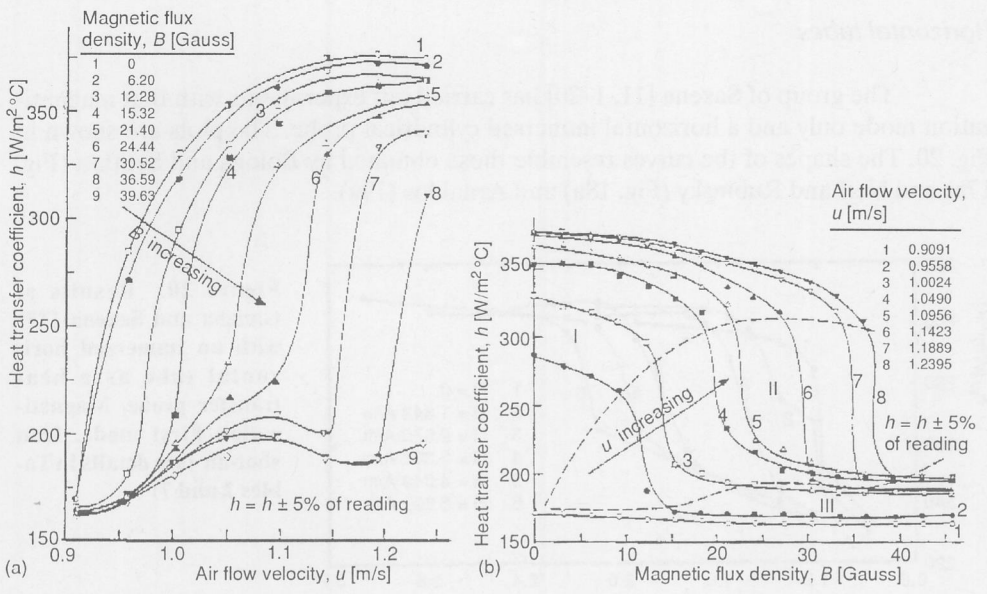

Figure 18. Neff and Rubinsky [16] data (See details in Tables 2 and 7)
(a) Magnetization FIRST mode; (b) Magnetization LAST mode

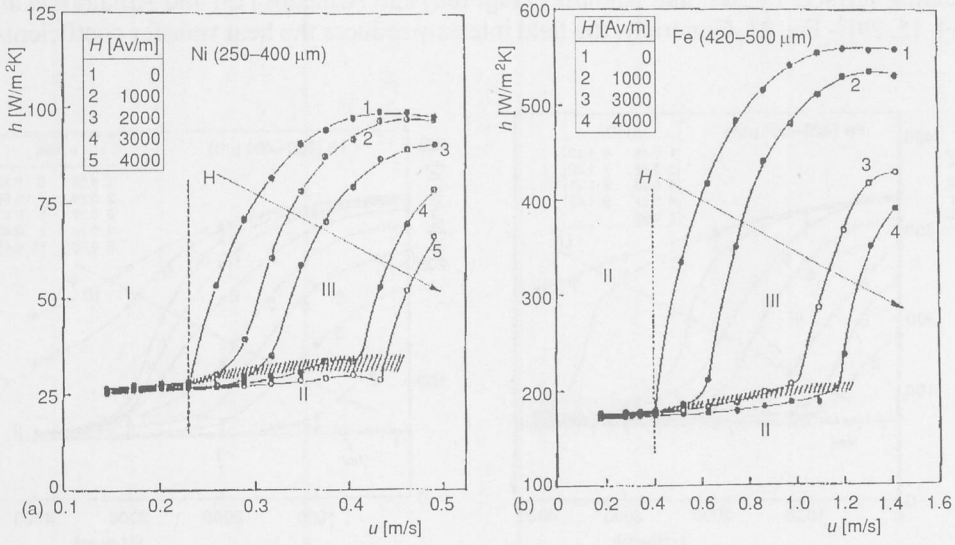

Figure 19. Arnaldos' results [13, 14, 29]. Adapted from [13]. By courtesy of J. Arnaldos. See details in Table 2 and 7 Magnetization FIRST mode (I – fixed bed; II – stabilized bed; III – fluidized bed). The present author adds the arrows

Horizontal tubes

The group of Saxena [11, 1–20] has carried out experiments with that magnetization mode only and a horizontal immersed cylindrical probe. The plots are shown in Fig. 20. The shapes of the curves resemble those obtained by Bologa and Syutkin (Fig. 17a) and Neff and Rubinsky (Fig. 18a) and Arnaldos (19a).

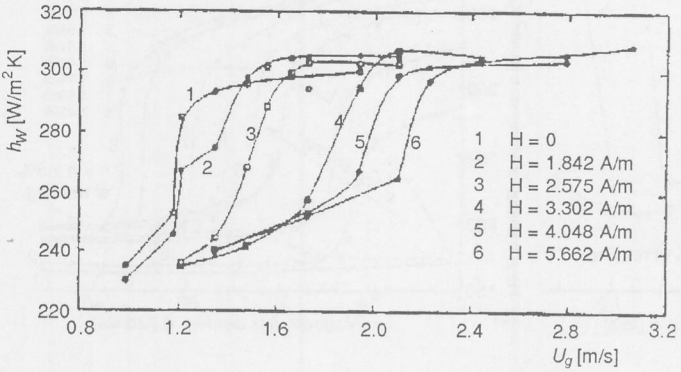

Figure 20. Results of Ganzha and Saxena [17] with an immersed horizontal tube as a heat transfer probe. Magnetization First mode. Iron shot-air (see details in Tables 2 and 7)

Magnetization LAST

The experiments carried out with that mode have been obtained with vertical heating surfaces by Neff and Rubinsky (Fig. 18b) and Arnaldos [13] and Arnaldos *et al.* [14, 15, 29] – Fig. 21. Generally, the field intensity reduces the heat transfer coefficients

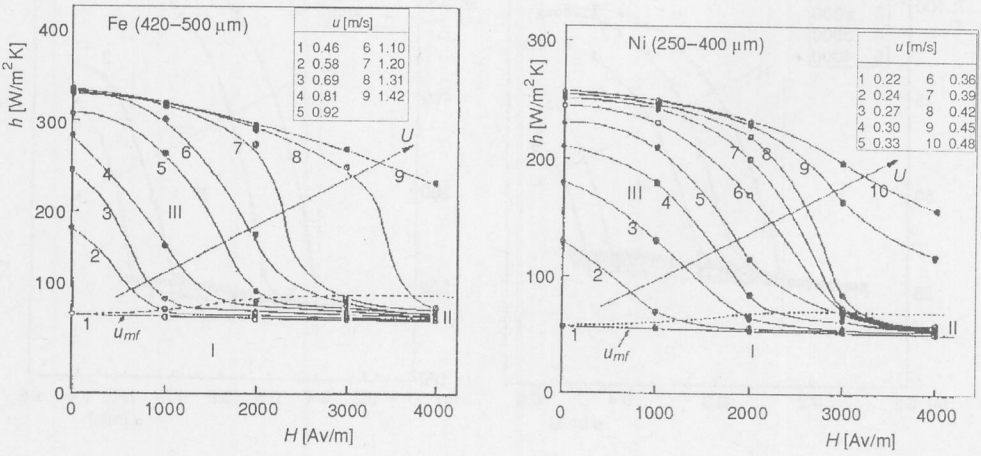

Figure 21. Arnaldos' [13, 14, 29]. Adapted from [13]. By courtesy of J. Arnaldos. See details in Tables 2 and 7. Magnetization LAST mode

despite the gas velocity. The higher values of h_w correspond to higher gas velocities and the non-magnetized fluidized beds exhibit the maximum heat transfer coefficients. Other authors have no performed experiments with that mode with steady magnetic fields. A special case of that mode is the application of an alternating magnetic field (f = 50Hz). The results shown in Fig. 22.

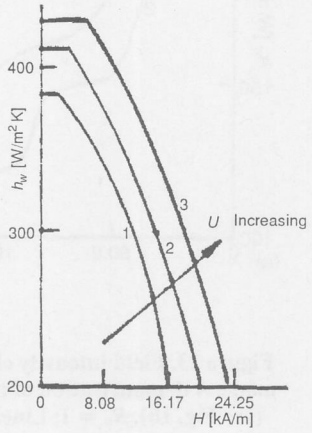

Figure 22. Heat transfer coefficient as a function of the field intensity of an alternating (time varying field of f = 50 Hz) axial magnetic field. Classified with the Magnetization LAST mode. Adapted from Zabrodsky and Tambovtsev [7]. (Original source – Fig. 3 in [7]). Lines: 1 – U = 0.39 m/s; 2 – U = 0.5 m/s; 3 – U = 0.66 m/s; The arrow was added by the present author

ON-OFF magnetization mode

The ON-OFF magnetization mode demonstrates results that may be related with caution to that exhibited by the Magnetization LAST mode. The reason of that assumption is the fact that during the ON period the field is applied on a preliminarily fluidized bed. In fact, the fluidized system passes very quickly through all the regimes already demonstrated by the Magnetization LAST mode [2, 38] under the action of an incrementally increasing steady magnetic field. The magnetic field creates intermittently a non-magnetized fluidized bed and a frozen bed [2, 38]. The corresponding heat transfer coefficients also alternate between minimum and maximum like in the case of a steady field created beds with Magnetization LAST mode. The results shown in Fig. 23 demonstrate this cyclical change of the heat transfer coefficient with the increased field strength. Moreover, in both cases the heat transfer coefficient- field intensity relationship exhibits a significant hysteresis that may be attributed to the hysteresis of the particle rearrangement (see Fig. 2 in [7] – not shown here).

The simultaneous effect of the gas flow rate and the frequency of the magnetization field (see the definition on Fig. 1a) is shown on Fig. 24. The plot indicates that the curves exhibit maxima like in the case of the magnetization FIRST mode (see the curves of Bologa and Syutkin, Neff and Rubinsky and Arnaldos). The increase of the frequency of the magnetization (*i.e.* the increase of the time of the field action on the particles) reduces the heat transfer coefficients. It should take into account that Fig. 24 shows results that practically do not exibit significant differences between the values of h_w obtained

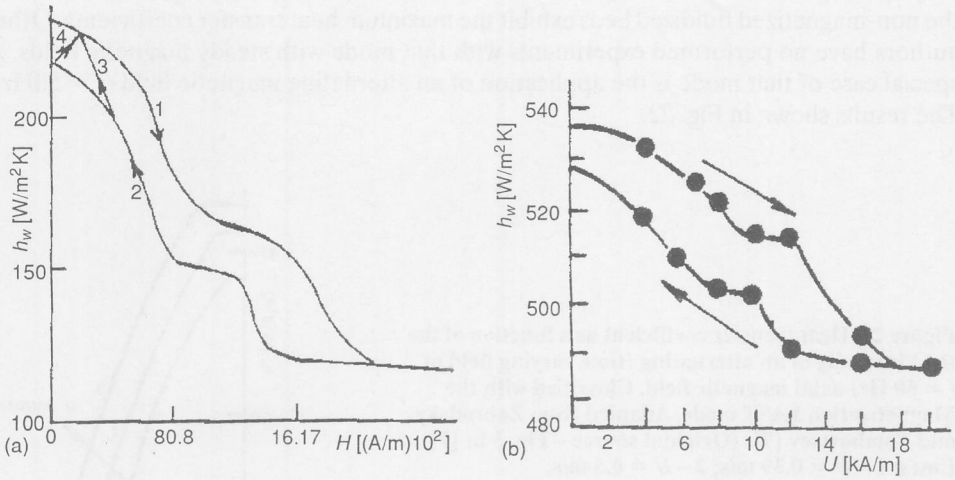

Figure 23. Field intensity effect on the heat transfer coefficient with ON-OFF magnetization mode. A demonstration of the hysteresis effect under the action of a pulsed field of f = 50 Hz (see Fig. 1b), R_o = 1; Lines: 1 – increasing field intensity (ON period), 2 – decreasing field intensity (OFF period)

(a) Results of Zabrodsky and Tambovtsev [7] (original source – Fig. 1 in [7]) U = 0.66 m/s; (b) Results of Stepanchuk [9] (original source Fig. 3 in [9]). U = 0.68 m/s. For additional details see Tables 1, 2 and 7

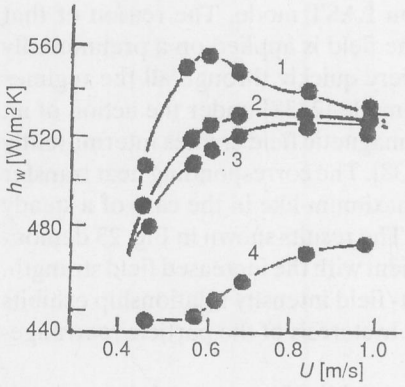

Figure 24. Results of Stepanchuk [9] (original Fig. 1 in [1]). Simultaneous effect of the gas velocity and the shape of the magnetization pulses and the frequency of magnetization.

Lines: 1 – zero field intensity, ON-OFF magnetization (H = 20 kA/m), Rectangular pulses (Fig. 1a); 2 – f = 6 Hz; 3 – f = 6 Hz and semi- sinusoidal pulses (Fig. 1b), 4 – f = 50 Hz

under magnetizations with f= 6 Hz and f = 3Hz. In both cases R_o= 1 (see Table 1). However, at R_o = 1 the magnetization at f = 50 Hz significantly reduces the values of h_w (practically there is no maximum). On the other hand the field intensity (Fig. 25) has the same effect like in the magnetization FIRST mode, *i.e.* the increase of H leads to reduced values of h_w at a fixed frequency of magnetization. Despite this the heat transfer coefficients increases parallel to the gas velocity.

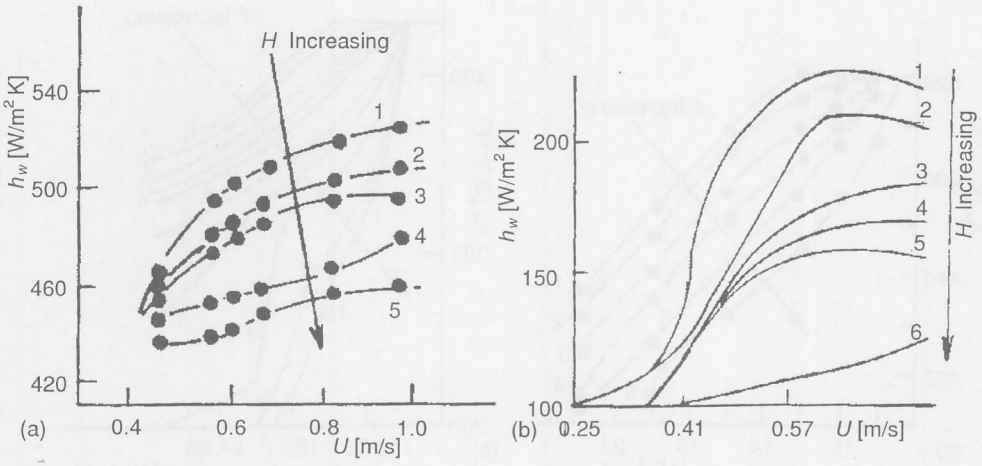

Figure 25. Simultaneous effects of the field intensity and the gas flow rate on the heat transfer coefficient with the ON-OFF magnetization mode. Pulse shapes in accordance with Fig. 1b, f = 50 Hz. The lines demonstrate the field intensity effect

(a) Stepanchuk [9] (Original Fig. 2 in [9], Lines (H, kA/m): 1 – 8, 2 – 10; 3 – 12; 4 – 50; 5 – 80
(b) Zabrodsky and Tambovtsev [7] (Original Fig. 4 in [7]). Lines (H, kA/m): 1 – 0; 2 – 6.06; 3 – 8.08; 4 – 10.1; 5 – 12.1; 6 – 52.5

The plots on Fig. 26 show the opposite situations, *i.e.* the simultaneous effect of the magnetization frequency and the field intensity on hw at a fixed gas velocity.

All the results reviewed above concern average in time values of the heat transfer coefficients between the bed and an immersed probe generating a constant heat flux. Unique unsteady-state experiments have been carried out by Stepanchuk [10] by cooling a steel sphere in a bed fluidized by a gas at ambient temperature. The results are shown on Fig. 27. The sphere temperature has been measured by thermocouple at the centre (r/R = 0). The heat transfer coefficient has been obtained by the relationship

$$h = h_0\left(1 - \frac{C_p m \rho tg\varphi}{3F_s k}\right)^{-1} \tag{10a}$$

where

$$h_0 = \frac{tg\varphi\rho C_p R}{3} \tag{10b}$$

in accordance with the theory of the h–calorimetry (in the Russian literature the term is α– calorimetry) [41]. All the symbols represent the properties of the steel sphere (see further Table 8).

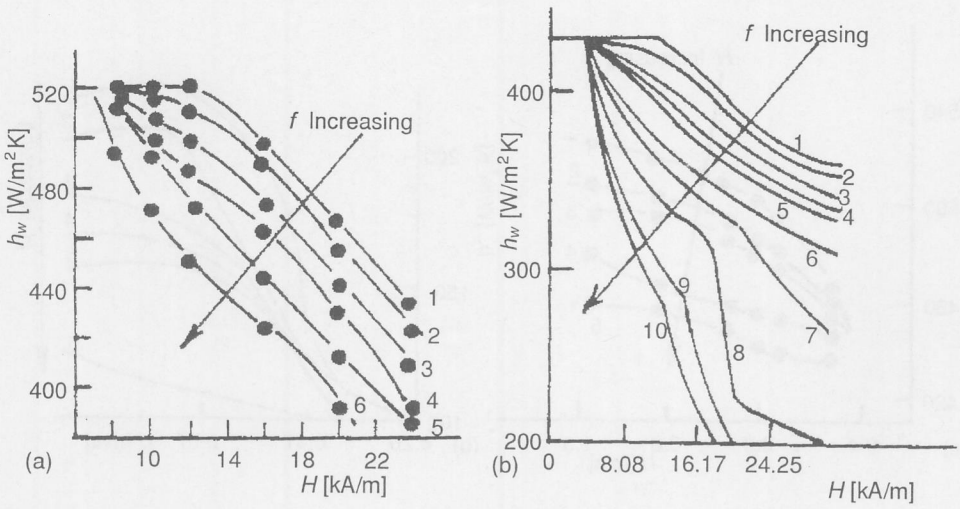

Figure 26. Simultaneous effect of the field intensity and the frequency of magnetization on the heat transfer coefficient with the ON-OFF magnetization mode at a fixed gas flow rate (Details in Tables 1, 2 and 7)

(a) Stepanchuk [9] (Original Fig. 4 in [9]). U = 0.68 m/s. Rectangular pulses (Fig. 1a): 1 – non-magnetized bed; 2 – f = 3 Hz; 3 – f = 6 Hz; 4 – f = 8 Hz; 5 – f = 12 Hz and 6 – f = 22 Hz.

(b) Zabrodsky and Tambovtsev [7] (Original Fig. 3b in [7]). U = 0.66 m/s. Line 1 – preliminary magnetized particles in a steady field, but under the fluidization H = 0; Rectangular pulses (Fig. 1a), f [Hz]: 2 – 2; 3 – 5; 4 – 7; 5 – from 10 to 15; 6 – 20; 7 – 25; 8 – 33, Semisinusoidal pulses (Fig. 1b); 9 – f = 40 Hz, 10 – 50 Hz

Table 8. Data used in the correlations (average values)

Substance / Properties	Air (323 K)	Steel	Steel shot & Steel powder	Reference
ρ [kg/m³]	1.03	7800	7800	[43, 44, 52]
μ [Pa·s]	$19.6 \cdot 10^{-6}$	–	–	[52]
k [W/mK]	$2.83 \cdot 10^{-2}$	60	60	[52]
Ms [kA/m]	–	1760	1 760	[43, 44]

The approximate calculations of the Biot number, Bi, (by means of the data shown on Fig. 27c) give variations of Bi with the frequency and the gas velocity (lines 2–3) in the range of 0.033 to 0.047. On the other hand, the fourfold increase of the field intensity (line 4) and the change of the type of the magnetization pulse from rectangular to semi-sinusoidal gives Bi in the range 0.013 – 0.033. Unfortunately, no data concerning

Bi are available in [10], so the conclusions are tentative due the readings of the graphs in [10]. The above estimations were done in the present paper by means of the temperature response curves constructed for spheres in [42] (Fig. 9.13 in [44] at $r/R = 0$). However, all the information presented on Fig. 27 indicates that the corresponding Fourier number varies in the range of 10 to 50.

Generally, the results shown on Figs. 24–27 indicate that the increase of the frequency at H = const or vice versa leads to the deceleration of the particles that reflects in the bed temperature field and bed-to surface heat transfer. The increase of the fluidizing gas flowrate eliminates slightly these effects due the increasing gas and particle convection effects.

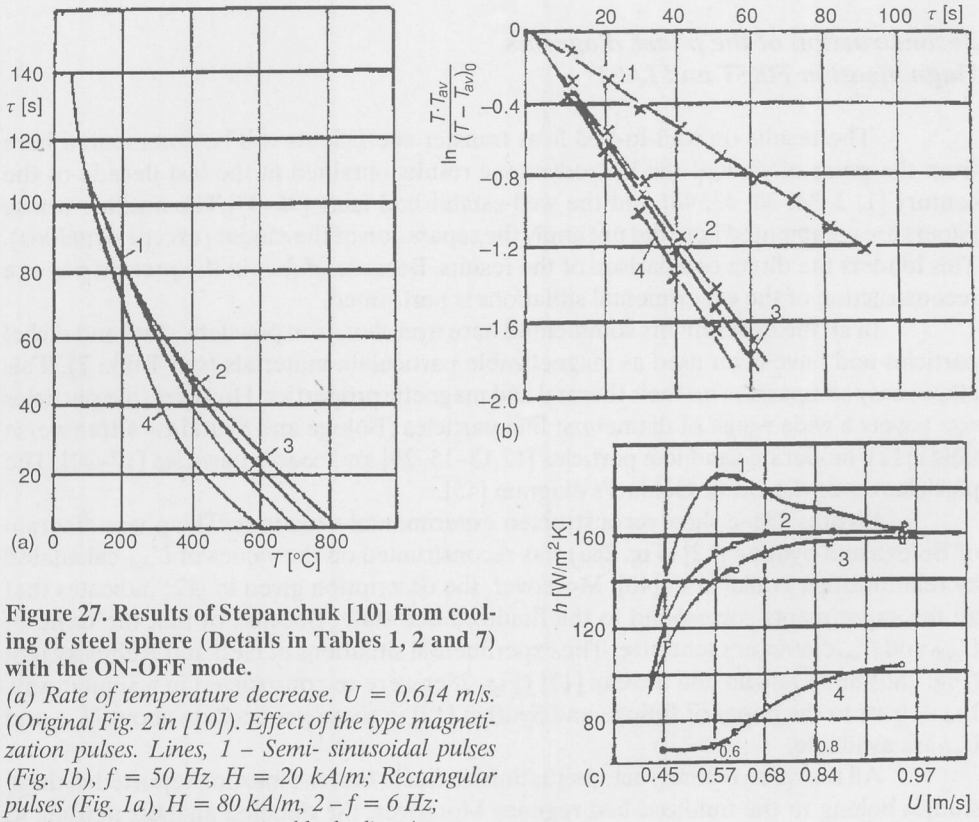

Figure 27. Results of Stepanchuk [10] from cooling of steel sphere (Details in Tables 1, 2 and 7) with the ON-OFF mode.

(a) Rate of temperature decrease. U = 0.614 m/s. (Original Fig. 2 in [10]). Effect of the type magnetization pulses. Lines, 1 – Semi- sinusoidal pulses (Fig. 1b), f = 50 Hz, H = 20 kA/m; Rectangular pulses (Fig. 1a), H = 80 kA/m, 2 – f = 6 Hz; 3 – f = 3 Hz. Non-magnetized bed – line 4.

(b) Semi-logarithmic plots demonstrating a regular regime of heat transfer betwwen the sphere and the bed. U = 0.614 m/s. Lines like in Fig. 27a.

(c) Variations of the heat transfer coefficient with the gas velocity. Effects of the type of magnetization pulses. Lines: 1 – Non-magnetized bed; Rectangular pulses (Fig. 1a), H = 20 kA/m; 2 – f = 6 Hz; 3 – f = 3 Hz. Semi-sinusoidal pulses (Fig. 1b) f = 50 Hz, H = 80 kA/m (Fig. 27. is a copy of the original Fig. 2 given in [10])

Reconstruction of the experimental conditions

Comments on the data before the further analysis

The data reviewed above strongly indicated that the hydrodynamics conditions have not been reported correctly in all the studies. The classification of the results in accordance with the three magnetization modes discussed here requires a correlation with the existing bed regimes (corresponding to the modes). Thus, the further analysis needs (see Figs. 1–2) detailed reconstructions of the experimental situations on the basis of the data available.

Reconstruction of the phase diagrams Magnetization FIRST and LAST

The results on wall-to-bed heat transfer coefficients will be commented here from the point of view of the hydrodynamic results obtained in the last decade of the century [1, 2, 34, 38, 43, 44] and the well-established facts [35–37].The authors whose papers are commented here did not apply the separation of the modes (except Arnaldos). This hinders the direct comparison of the results. Because of that in the present paper a reconstruction of the experimental situations is performed.

In all the experiments commented here iron shot, iron powders, steel and nickel particles and have been used as magnetizable particulate materials (see Table 7). This allows easy comparison on their thermal and magnetic properties. However, the particles size covers a wide range of diameters: fine particles (Bologa and Syutkin – a transverse field) [12], moderate sand like particles [12,13–15, 29] and coarse particles [17–20]. The particles cover the entire Geldart's diagram [45].

Figures 28a–c show reconstructed experimental situations. The phase diagram of Bologa and Syutkin [12] (Fig. 28a) was reconstructed on the values of U_{mf0} calculated by relationships available in [46]. Moreover, the description given in [12] indicates that all the experiments correspond to the fluidized bed state. Because of that the trend of U_{mf0} and U_{mf} curves are tentative. The experimental situations of Neff and Rubinsky [16] (Fig. 28b) and Ganzha and Saxena [17] (Fig. 28c) were re-constructed in a similar way. In contrast to the paper of Bologa and Syutkin [12] in these papers data about U_{mf0} and U_{mf} are available.

All the three reconstructed situations indicate that the maxima reported in these studies belong to the fluidized bed regimes Moreover, the detailed analysis permits to detect the values of h_w in the regime of MSB (see below).

The experimental situation of Neff and Rubinsky [16] corresponding to the magnetization LAST mode is shown on Fig. 29. The whole knowledge on the bed behaviour available with that magnetization mode was applied [2, 38]. The reconstructed data confirm again that the maximum heat transfer coefficients belong to the zones with negligible effects of the field applied.

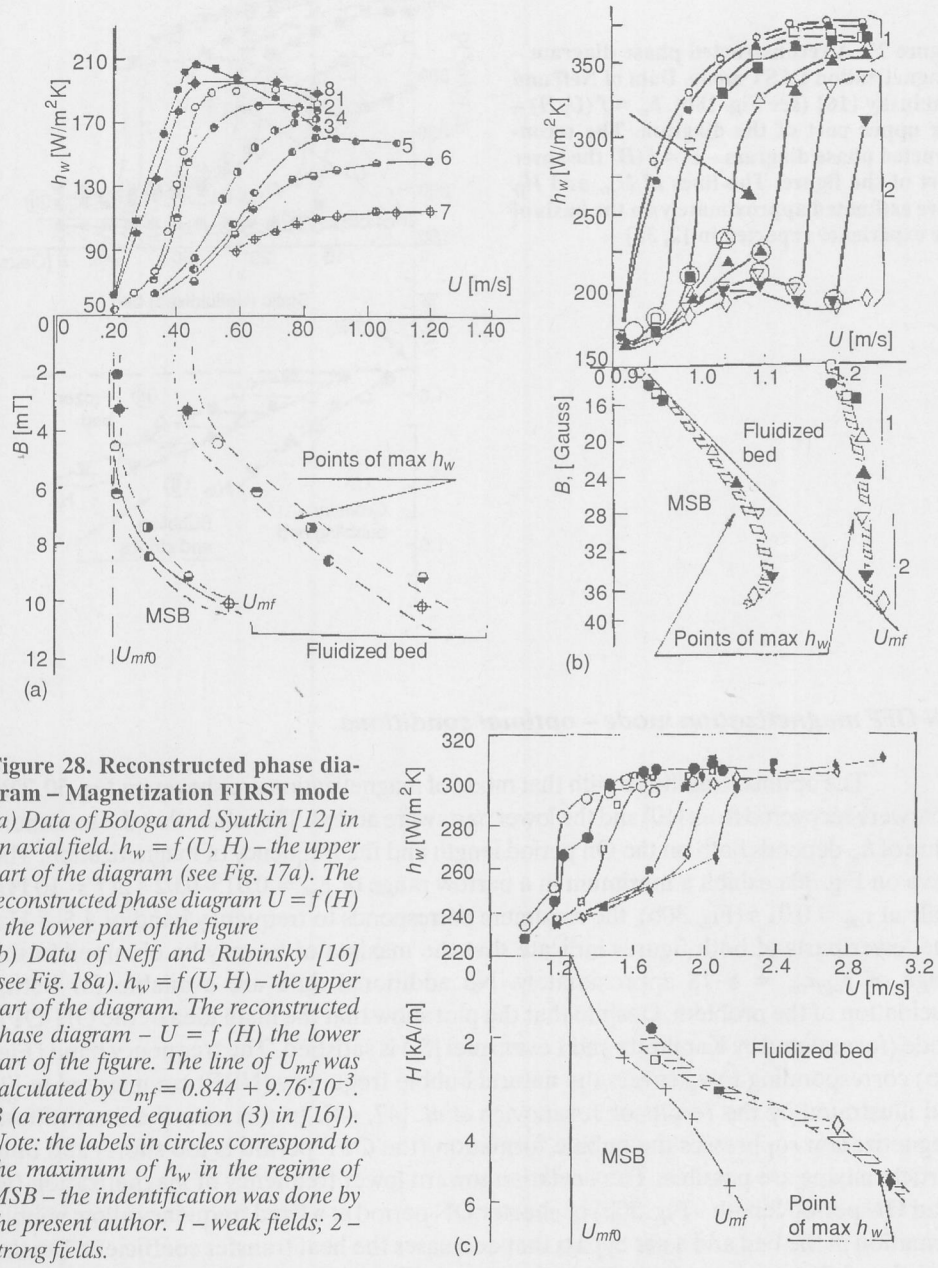

Figure 28. Reconstructed phase diagram – Magnetization FIRST mode
(a) Data of Bologa and Syutkin [12] in an axial field. $h_w = f(U, H)$ – the upper part of the diagram (see Fig. 17a). The reconstructed phase diagram $U = f(H)$ – the lower part of the figure
(b) Data of Neff and Rubinsky [16] (see Fig. 18a). $h_w = f(U, H)$ – the upper part of the diagram. The reconstructed phase diagram – $U = f(H)$ the lower part of the figure. The line of U_{mf} was calculated by $U_{mf} = 0.844 + 9.76 \cdot 10^{-3} B$ (a rearranged equation (3) in [16]). Note: the labels in circles correspond to the maximum of h_w in the regime of MSB – the indentification was done by the present author. 1 – weak fields; 2 – strong fields.
(c) Data of Ganzha and Saxena [17] (see Fig. 20). $h_w = f(U, H)$ – the upper part of the diagram. The reconstructed phase diagram – $U = f(H)$ the lower part of the figure. The lines of U_{mf0} and U_{mf} were found out from various figures available in [17]

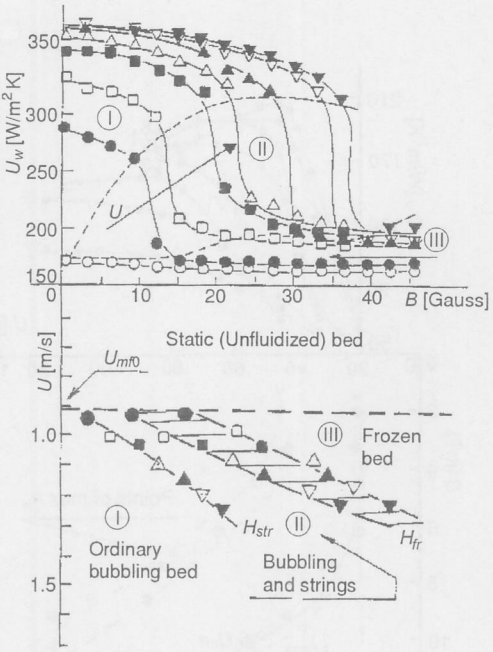

Figure 29. A reconstructed phase diagram – Magnetization LAST mode. Data of Neff and Rubinsky [16] (see Fig. 18b). $h_w = f(U, H)$ – the upper part of the diagram. The reconstructed phase diagram – $U = f(H)$ the lower part of the figure. The lines of H_{str} and H_{fr} were estimated approximately on the basis of the experience reported in [2, 38]

ON-OFF magnetization mode – optimal conditions

The optimal conditions with that mode of magnetization are shown on Fig. 30. The plots were recovered from [10] and the lower parts were added. They show that the maximum value of h_w depends both on the On period length and the frequency of magnetization. The curve on Fig. 30a exhibit a maximum in a narrow range of τ_{on} = 0.015–0.02 s at f = 10 Hz, while at τ_{on} = 0.01 s (Fig. 30b), the maximum corresponds to frequency band of 4.5–8 Hz. The lower parts of both figures indicate that the maxima of h_w may be obtained in the range of τ_{off}/τ_{on} = 8–18 approximately. No additional data are available for better elucidation of the problem. Despite that the plot show that the main idea of the ON-OFF mode (formulated by Kamholtz and Levenspiel [5]) is satisfied. The frequency band (Fig. 30b) corresponding to h_w covers the natural bubble frequency (NBF) commented in [2] and illustrated by the results of Jovanovich *et al.* [47, 48]. In this case the intermittent magnetization suppresses the bubble formation (the OFF period is too short) and only particle mixing are possible. The deviation toward lower frequency of magnetization (at fixed ON period length – Fig. 30b) or shorter ON period at a fixed frequency allow bubble formation in the bed and a gas bypass that decreases the heat transfer coefficient. On the other hand the increase of the ON period length (Fig. 30a) or the frequency of magnetization (at τ_{on} = const) make the bed more difficult for fluidization. The later opinion is based on the fact that such conditions do not permit particle mixing and the bed behaves

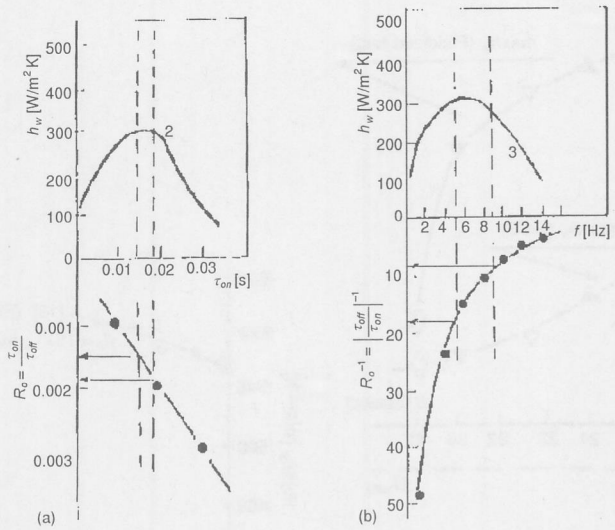

Figure 30. Optimal conditions with ON-OFF magnetization modes. Data of Stepanchuk [10]. (Original Figs. 3 and 4 in [10]). Magnetite-Air (see Table 1). The original data are redrawn (the lines corresponding to the pure magnetic particles only) as the upper parts of the figures. The present author on the basis of the data summarized in Table 1 designed the lower parts.
(a) h_w as function of the ON period length (τ_{on}) at $f = 10$ Hz.
(b) h_w as a function of the frequency of magnetization at $\tau_{on} = 0.01$ s

like MSB (Magnetization FIRST) or a frozen bed (Magnetization LAST) [2, 38]. The fixed bed behaviour exhibited by both regimes leads to significant temperature gradients (see for example the data commented in point 3).

The field intensity effect on the heat transfer coefficient with ON-OFF mode is the same like in the other two modes created by steady state or time-varying fields. In all the cases the increasing field intensity aggregates the particles and decreases their mobility. The range of the intensities depends on the properties of the particles used (see comments in [2]).

Maximum heat transfer coefficients – comments

● *Magnetization FIRST mode – a stabilized bed*

The maximum heat transfer coefficients ($maxh_w$) are shown in Figs. 31a, b. The values were extracted from various original plots by digitazing (see the figure captions) and by means of the reconstructed phase diagram. Both figures show that the curve of $maxh_w$ corresponding to the stabilized bed regime has two branches as a function of the field intensity. No comments exist in the published studies. The possible explanation may employ the fact that the increasing branch corresponds to the increasing bed porosity and

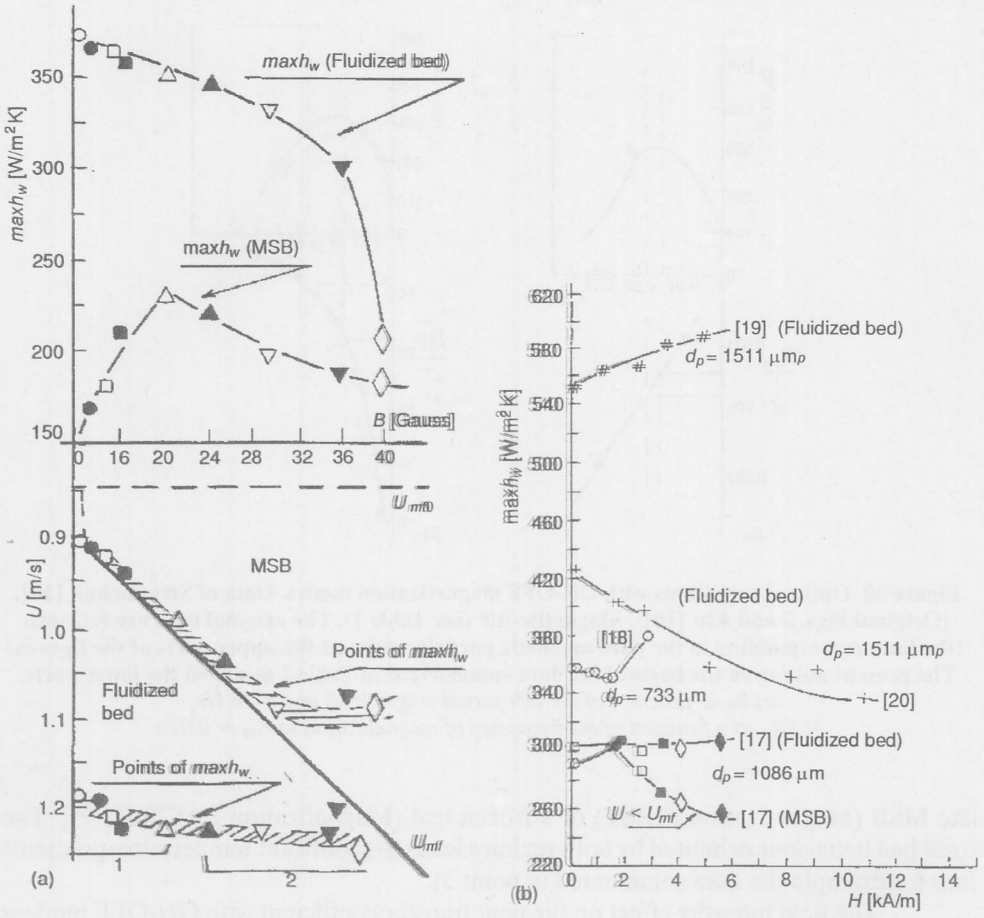

Figure 31. Maximum heat transfer coefficients (total values). Data corresponding to the magnetization FIRST mode

(a) Maximum h_w corresponding to the results of Neff and Rubinsky [12] (vertical heat probe). See the lower part of the figure with the reconstructed phase diagram. 1 – weak fields; 2 – strong fields
(b) Maximum h_w obtained by horizontal tube probes. Data extracted from teh results of Ganzha and Saxena [17] (Source: Fig. 6 in [17]) (see the symbols used on Fig. 28c), Saxena and Dewan [20] (Source: Fig. 2 and 3 in [20]), Dolidovich et at. [19] (Source: Fig. 3d in [19]) and Qian and Saxena [18] (Source: Fig. 2–5 in [18]

the increasing gas convection affects the value of $maxh_w$. As already mentioned the stabilized bed has a fixed beds structure affected by the field applied, so the decreasing branch may be attributed to the anisotropy of the particle arrangement along the field lines (axial field only applied) and the channels dividing the particle aggregates. In this case the gas bypass through the channels decreases the heat transfer efficiency. The situations with the two types of the probe surface – a vertical probe (Fig. 31a) and a

horizontal tube (Fig. 31b) are similar. Therefore, the bed expansion has a limit separating the well-expanded bed and the anisotropic structure with channels. However, the expansion of a particular system (particles-field orientation-field intensity) depends on many factors. No data considering the heat transfer from that point of view are available in the literature.

● *Magnetization FIRST mode – a fluidized bed*

The data available about $maxh_w$ in the fluidized bed regimes indicate that there are concurrent actions of the fluid flow and the magnetic field. The field aggregates the particles (*i. e.* enlarge the size of the fluidized particles) and decelerates their motions. Both effects decrease the values of the heat transfer coefficients. They may be related to the well-known results on the particle size effect on $maxh_w$ in non-magnetic beds [3, 4]. Both field effects may be considered as negative on the surface-to-bed heat transfer in a magnetic field.

The fluid flow has the opposite role. The data available do not allow easy detection of the contributions of both actions on the heat transfer. The maxima in the curves of Neff and Rubinsky (Fig. 18a, Fig. 28b-top and Fig. 31a-top) correspond to a very narrow velocity range that explains the decreasing $maxh_w$ with the field intensity. On the other hand the results of Saxena's group (Fig.20, Fig. 28c. and Fig.31b) span a wide range of gas velocities. The latter results clearly demonstrate that the increasing gas velocity may compensate the negative effect of the field intensity.

However, the plots on Fig. 31b demonstrate some contradicting tendencies. All the data have been obtained under practically equal condition (one and the same column and a heat transfer probe) but with slightly different coarse particles of iron shot. There is no explanation of the different behaviour exhibited by the curves. Generally, the data of Saxena and Dewan [20] and those of Qian and Saxena [18] (in a limited range of field intensities) confirm the trend demonstrated by the results of Neff and Rubinsky [16] and the comments done above. On the other hand the results of Ganzha and Saxena [17] (a weak dependence on H) and these of Dolidivich *et al.* [19] demonstrate just the opposite behaviour as a function of the field intensity. Moreover, the Dolidovich *et al.* [19] and Saxena and Dewan [20] have performed the experiments with one and the same particulate materials. No particle size effect on $maxh_w$ is detectable at $H = 0$ in agreement with the well-established classic results [3, 4], while the slopes of both curves are opposite. Particle size effect (at $H = 0$) on $maxh_w$ may be found in the lower part of Fig. 31b despite the fact that the curve of Qian and Saxena does not confirm the general tendency. It should be noted that the data shown on Fig.31b do not demonstrate the implicit effect of the gas velocity and the bed structure formed.

The field orientation effect is not detectable on the basis of the data available since only those of Bologa and Syutkin have been reported. The heat transfer coefficients on Fig. 17b are twice greater that all the other obtained in axial fields. However, it is not clear what is the reason for that: the smaller particle size like in conventional beds [3, 4] or the transverse field orientation avoiding the channelling [34, 44].

- *Magnetization LAST mode*

As mentioned, the field decreases the particle mobility and increase the aggregate sized with that mode of magnetization. The maximum heat transfer coefficients corresponds to the regimes where the field effects are not significant (see the initial section of the zones I on Figs. 18b and 21). The further increase of field, *i. e.* the development of the bed structure toward that of a fixed bed (a frozen bed [2, 38]) reduces several times the heat transfer coefficients. The values of $maxh_w$ are similar to these observed in the regime of MSB (high field intensity) where the gas bypassing through the channels takes place. Therefore, the Magnetization LAST mode is not successful approach for a heat transfer regulation. The main reason is the use of a steady magnetic field that forms stable aggregates. No investigations have been performed in a transverse magnetic field where the particle aggregates are fragile and easy controllable by the fluid flow (see for example [2, 38]).

- *ON-OFF magnetization mode*

As commented in section under the title ON-OFF magnetization mode – optimal conditions, the ON-OFF mode may be considered as a pulse modification of the magnetization LAST mode. The bed quickly shifts the state- between a non-magnetized state and the frozen bed. The results of Stepanchuk [10] (Fig. 30) show that it should be a balance between the On and Off periods. Unfortunately, the frequency of magnetization employed by Stepanchuk and Zabrodsky and Tambovtsev are approximately 100 times higher (see Table 1) that used by Kamholtz and Levenspiel (the field is steady during the On period). This does not allow a direct correlation of the results on the temperature distribution and the heat transfer coefficients with that magnetization mode. The problem is practically non-investigated, but offers a large area for future studies and applications.

Maximum heat transfer coefficients – data correlations

The data available indicate that the magnetic field permits easy control of bed--to-surface heat transfer. Unfortunately the lack of complete data hinders an unified approach for data correlations. For example Saxena et al. have correlated the data by the relationship [49] based on the mechanistic theory of Ganzha [50] for large particle fluidized beds:

$$\mathrm{Nu} = 8.95(1-\varepsilon)^{2/3} + C\,\mathrm{Re}^{0.8}\,\mathrm{Pr}^{0.43}(1-\varepsilon)^{0.133}\varepsilon^{-0.8} \qquad (11)$$

where C is related to the powder classification of Saxena and Ganzha [51].

It was demonstrated in [11, 7, 20] that for stabilized beds $C = 0.085$ [11, 17, 20] while for fluidized beds [11, 17] $C = 0.17$. The analysis of Ganzha [50] shows that the coefficient 8.95 of first term of Eq.11 may be replaced by $8.5\,k_{gp}$, where k_{gp} is

$$k_{gp} = \frac{1}{3.4\left(\frac{k_g}{k_p}\right) + 0.94} \tag{12}$$

The final equation employed in [11,17,20] is

$$\mathrm{Nu} = 8.5 k_{gp}(1-\varepsilon)^{2/3} + C\,\mathrm{Re}^{0.8}\,\mathrm{Pr}^{0.43}(1-\varepsilon)^{0.133}\varepsilon^{-0.8} \tag{13}$$

However, in order to overcome the problem with reliable data on ε variations in MSB regime a simplified form has been proposed [17]:

$$\mathrm{Nu} = \frac{h_w d_p}{k_g} = 0.116\,\mathrm{Re}^{0.8} + 5.57 \tag{14}$$

developed for air-iron and air-iron/sand systems.

The studies reviewed in the present paper have a common disadvantage; *i.e.* the lack of data considering the ε variations in the frames of the heat transfer experiments carried out. In order to overcome the problem the data summarized were correlated by the relationship

$$\mathrm{Nu} = \frac{h_w d_p}{k_g} = A_0\,\mathrm{Re}^m\,S_0 \tag{15}$$

$$S_0 = \mathrm{Pr}^{0.8}\sqrt{\mathrm{Ar}}\left(\frac{k_g}{k_p}\right)\left(1-\frac{H}{M_s}\right) \tag{16}$$

The term S_0 contributes simultaneously the particle size effect (via the Arhimedes number), and field effects by the dimensionless field intensity H/M_s (introduced in [34]; see also Fig. 5d in [2]). The proposed equation is an alternative version between the correlations available for nonmagnetic fluidized beds [3, 4] (in this case the last term is equal to 1) and the situation of a deficiency of data from the experiments reviewed.

The data considered for correlation corresponds to the fluidized regime only. In order to eliminate the lack of data concerning the thermophysical properties of the gas and the particles used in the particular experiments the results were correlated with the data summarized in Table 8. The experiments performed with steel and iron particles have been correlated only due to reliable data on the heat transfer coefficients available in the referred papers.

The data plotted on Fig. 32 and the established coefficients demonstrate two tendencies (key to Fig. 32 is given in Table 9). The better results were obtained with the

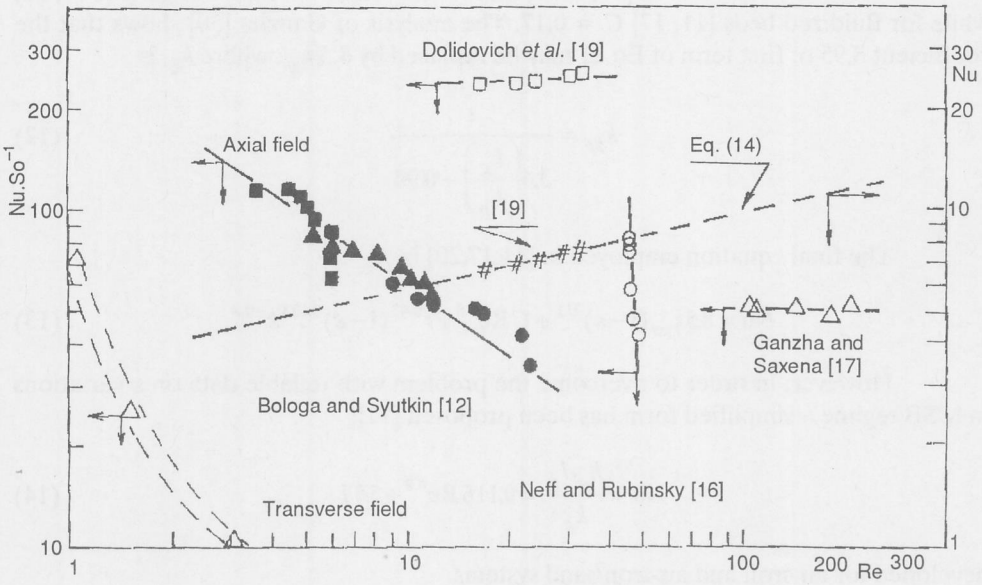

Figure 32. Plots of the data from various sources. The solid lines correspond to Eq. 15. The keys are summarized in Table 9

Table 9. Coefficients of Eq. (15) and key to Fig. 32
Additional information is available in Table 7

Reference	Key and particle size d_P [μm]	A_0	m	R^2	Exp. Points
Bologa and Syutkin [12] axial field	■ – (160–200); ▲ – (200–250); ● – (250–325)	239.6	–0.586	0.887	24
Bologa and Syutkin [12] transverse field	△ – (0–90)	57.042	–1.488	0.9853	4
Neff and Rubinsky [16] axial field	○ – 727	!	!	!	10
Dolidovich *et al.* [19] axial field	□, # – 1511	192.22	0.0782	0.864	5
Ganzha and Saxena [17] axial field	△ – 1086	55.56	–0.02	0.055	6

! The data do not allow a correct correlation due to the practically equal values of U corresponding to various $maxh_w$ (See Fig. 18, 28a-top)

data of Bologa and Syutkin [12] obtained in an axial field. The ratio (Nu/S_0) decreases with the increase of the Reynolds number, but the higher values of (Nu/S_0) correspond to finer particles that confirm the well-known results. The variations with Re (*i.e.* the decreasing tendency) demonstrate by an implicit manner the field effect on the heat transfer coefficient. The higher field intensities need higher gas velocities (Re respectively), but lead to lower heat transfer coefficients due to the particle aggregation. The same tendency is exhibited be the results of Neff and Rubinsky [16] and those of Arnaldos *et al.* [13–15] (not shown here). Remember that all these data have been obtained with vertical heat transfer probes.

On the other hand, just the opposite tendency is exhibited by the results of Saxena's group [17, 19] obtained by a horizontal cylindrical probe. In fact, the simultaneous effects of field and the gas velocity on (Nu/S_0) are slightly detectable in these results. The plot of Eq. (14) on the same figure demonstrates a very simplified correlation that does not take into consideration the field effects. The similarity between the plots of Dolidovich's results presented by both correlations is due to the fact that within the field intensity range employed the term ($1 - H/M_s$) is practically equal to 1 like in the absence of a field. The situation in [17] is similar (see Table 7 for the range of H and Table 8 for the value of M_s).

FINAL COMMENTS

The paper went through various experimental situations performed with magnetically controlled gas fluidized beds. The heat transfer characteristics were collected and discussed from different studies carried out at random and from different point of view. The unified approach employed here allows easy detection of the field orientations and magnetization mode impacts on the heat transfer characteristics. The analysis done permits several short conclusions:

- The stabilized beds exhibit thermal behaviour that completely coincides with the thermal characteristics of ordinary packed beds. Significant axial and radial temperature profiles due to the particle immobilization by the induced interparticle forces.
- The ON-OFF technique is an alternative magnetization approach that overcomes the problems with the significant temperature gradients.
- The data available indicate that the magnetic field permits an easy control of bed–to-surface heat transfer. Unfortunately, the lack of data hinders the establishment of a complete picture of the heat transfer process. The reconstruction of the experimental conditions done clarifies them approximately. The values of A and m listed in Table 3 indicate that the measured data are not enough for a correct data correlations.
- The further experiments should be carried out carefully in order to establish the correct relationship between the regime created and the heat transfer coefficient. The size of particle aggregates should be taken into account too.

NOMENCLATURE

Ar – Archimedes number, $\mathrm{Ar} = d_p^3 \rho_p (\rho_p - \rho_g) g / \mu_g^2$
B [T] – magnetic field induction
Bi – heat transfer Biot number, $\mathrm{Bi} = hR/k$
C – a dimensionless constant (Eq. 11)
C_p [J/kg K] – specific heat capacity (Eq. 10)
D_c [m] – column diameter
D_s [m] – internal diameter of the magnetic system
d_b [cm] – bubble diameter (a symbol used by Jovanović and co-workers)
E – relative bed height, $E = (h_b - h_{b0})/h_{b0}$
F – a parameter defined by Eq. (8)
Fo – Fourier number, $\mathrm{Fo} = \alpha\tau/R^2$
F_s [m^2] – the surface of the sphere (Eq. 10)
f [Hz] – frequency
g [m/s^2] – gravitational constant
H [A/m] – magnetic field intensity
H_{str} [A/m] – magnetic field intensity at which particle "strings" emerged (see comments in [2, 38])
H_{fr} [A/m] – freezing field intensity, (see comments in [2, 38])
h_b [m] – bed height
h_{b0} [m] – initial bed height
h [W/m^{2}K] – heat transfer coefficient
h_0 [W/m^{2}K] – heat transfer coefficient defined by Eq.10b
h_w [W/m^{2}K] – heat transfer coefficient between the bed and an immersed surface defined by Eq. 9
$maxh_w$ [W/m^{2}K] – maximum heat transfer coefficient between the bed and an immersed surface
k [W/m K] – thermal conductivity
k_b [W/mK] – effective thermal conductivity of the bed
L [m] – axial distance along the particle bed
L_c [m] – fluidization column length
L_s [m] – height of the magnetic system used
M_s [A/m] – magnetization at saturation
m [kg] – mass (see Eq. 10)
Nu – Nusselt number
Q [W] – total heat power
q [W/m^2] – heat flux per unit area of the heater
$\dot{q}$ [W/m^{2}s] – heat transfer flux rate
R [m] – sphere radius (Eq. 10)
R_e – particle Reynolds number, $\mathrm{Re} = \rho_p U d_p / m_g$
Ro – ratio of the pulsed field periods with the ON-OFF mode, $\mathrm{Ro} = \tau_{off}/\tau_{on}$
r [m] – radial coordinate

r_c [m] – column radius
Δr [m] – difference of radial coordinates
S [m^2] – heater surface
S_0 – a term defined by Eq. (16)
T [K or °C] – temperature
T_w [K] – surface temperature of the probe wall
T_b [K] – fluidized bed average temperature
T_0 [K] – room temperature,
ΔT [K or °C] – temperature difference
ΔT_r [K or °C] – radial temperature difference
tgφ – the slope of the lines on Fig. 27b
U [m/s] – superficial gas velocity
U_{mf0} [m/s] – minimum fluidization velocity in the absence of a magnetic field
U_{mf} [m/s] – minimum fluidization velocity at $H > 0$
z [m] – axial coordinate

Greek letters

α [m^2/s] – thermal diffusivity, $\alpha = k/\rho C_p$
γ [deg] – angle defining the direction of radial temperature measurements (Arnaldos' results)
δ_L – dimensionless axial position, $\delta_L = \Delta L/D_c$
ε – bed voidage
ρ [kg/m^3] – density
τ_{on} [s] – length of the magnetization period
τ_{off} [s] – length of the mixing period
θ [deg] – angular coordinate

Subscripts

Exp. – experimental
Calc. – calculated
g – gas
p – particle

REFERENCES

[1] Hristov, J. Y., Comments on Gas-Fluidized Magnetizable Beds in a Magnetic Field, Part 1: Magnetization FIRST Mode, *Thermal Science*, *2* (1998) 2, pp. 3–25
[2] Hristov, J. Y., Comments on Gas-Fluidized Magnetizable Beds in a Magnetic Field, Part 2: Magnetization LAST Mode and Related Phenomena, *Thermal Science, 3* (1999) 1–2, pp. 15–45
[3] Botterill, J. S. M., Fluid-Bed Heat Transfer, Academic press, London, 1975
[4] Zabrodsky, S. S., Hydrodynamics and Heat Transfer in Fluidized Beds, M. I. T. Press, 1966

[5] Kamholtz, K., Enhancing Characteristics of Magnetically Stabilized Fluidized Beds, US Patent, 4 143 168, 1979
[6] Levenspiel, O., Kamholtz, K., Enhancing Characteristics of Magnetically Stabilized Fluidized Beds, US Patent, 4 272 893, 1981
[7] Zabrodsky, S.S., Tambovtsev, Yu. I., A Possibility of a Magnetic Control of the Heat Transfer between a Surface and a Ferromagnetic Fluidized Bed, *Vesti Acad. Nauk BSSR, Series of Physical and Energetic Sciences, 1* (1976), pp. 51–56
[8] Stepanchuk, A.V., Investigations on the Heat Transfer Between a Sphere and a Fluidized Beds with and without Application of a Magnetic Field. *Vesti Acad. Nauk BSSR, 1* (1981), pp.157–162
[9] Stepanchuk, A.V., On the Possibilities of Heat Transfer Process Control in a Ferromagnetic Fluidized Bed, Inst. Heat Mass Transfer, Belarus Acad. Sci., Minsk, pp. 136–141
[10] Stepanchuk, A.V., Peculiarities of the Heat Transfer in a Fluidized Bed of Ferromagnetic Particles with an External Magnetic Field, *Inst. Heat Mass Transfer, Belarus Acad. Sci.*, Minsk, (1984), pp. 110–114
[11] Saxena, S. C., Ganzha, V. L., Rahman, S. H., Dolidovich, A. F., Heat Transfer and Relevant Characteristics of Magnetofluidized Beds, *Advances in Heat Transfer, 25* (1994), pp.151–249
[12] Bologa, M. K., Syutkin, S. V., Magnetic Field Effect on the Heat Transfer in a Fluidized Bed, *Electronna. obrabotka materialov* (Russia), *6*, (1976), pp. 61–66
[13] Arnaldos, J., Estudi de l'estabilitzacio dels llits fluidizacio solid-gas mitjancant l'aplicacio d'un camp magnetic, Ph. D. Thesis, Univ. Politechnica de Catalunya, Barcelona, 1985
[14] Arnaldos, J., Puigjaner, L., Casal, J., Heat and Mass Transfer in Magnetically Stabilized Fluidized Beds, in: Fluidization V. (Ed., Ostergaard-Sorensen), Eng. Foundation, New York, 1986, pp. 425–432
[15] Arnaldos, J. Lazaro, M., Casal, J., The Effect of Magnetic Stabilization on the Thermal Behaviour of Fluidized Beds, *Chem. Eng. Sci., 42* (1987), pp. 1501–1506
[16] Neff, J., Rubinsky, B., The Effect of a Magnetic Field on the Heat Transfer Characteristics of an Air Fluidized Bed of Ferromagnetic Particles, *Int. J. Heat Mass Transfer, 16* (1983), pp. 1885–1889
[17] Ganzha, V. L., Saxena, S. C., Heat-Transfer Characteristics of Magnetofluidized Beds of Pure and Admixtures Magnetic and Nonmagnetic Particles, *Int. J. Heat Mass Transfer, 41* (1988), pp. 209–218
[18] Qian, R. Z., Saxena, S. C., Heat Transfer from an Immersed Surface in a Magnetofluidized Bed, *Int. Comm. Heat Mass Transfer, 20* (1993), pp. 859–869
[19] Dolidovich, A. F., Ganzha, V. L., Saxena, S. C., Rahman, S. H., The Magnetic Field Effect on the Particle Behaviour and the Heat Transfer Between an Immersed Horizontal Tube and a Gas magnetofluidized Bed, *Fluidization IX*, 1998, pp. 453–460
[20] Saxena, S. C., Dewan, S. S., Heat Transfer from a Horizontal Tube in a Magnetofluidized Bed, *Int. Comm. Heat Mass Transfer, 23* (1996), pp. 655–664
[21] Zrunchev I. A, On the Effective Stability of Fluidized Catalyst Bed in a Magnetic Field, *Ann. of UCTM*, Sofia, *22* (1975), 3, pp. 121–127
[22] Zrunchev I. A., Popova, T. F., Catalytic Processes in Magnetic Structured Catalyst Beds, New Trend of Catalysis, *Proceedings*, 8th Int. Congress on Catalysis, vol. *IV*, (1984), pp. 847–858, Berlin, Germany
[23] Zrunchev I. A., Popova, T. F., Catalytic Processes in Magnetic Structured Catalyst Beds, New Trend of Catalysis, *Proceedings*, 9th Int. Congress on Catalysis, vol. *2* (1984), pp. 246–253, Calgary, Canada
[24] Selwood, P. W., Magnetochemistry, McGraw Hill, New York, 1956
[25] Liemelzs, J., Morgan, J. P., Magneto-Catalytic Effect in Ethylene Hydrogenation Reaction, *Chem. Eng. Sci., 22* (1977), pp. 781–791
[26] Liemelzs, J., Aleman, H., External Magnetic Field Effect in Ethylene Hydrogenation Reaction over Nickel, Cobalt and Iron Catalyst, *Chem. Eng. J., 5* (1973), pp. 129–135
[27] Bozorth, R. M., Ferromagnetism, Van Nostrand, 1951
[28] Vissokov, G. P., Ivanov, D. G., Thermo-Magnetic Analysis of Catalysts for Ammonia Synthesis, *Ann. of UCTM*, Sofia, *22* (1975), 3, pp. 181–189
[29] Casal, J., Arnaldos, J., Heat and Mass Transfer in Magnetized Fluidized Beds, *Trends in Heat, Mass and Momentum Transfer, 1* (1991), pp. 153–166
[30] Aerov, M. E., Todes, O. M., Hydraulic and Thermal Fundamentals of the Operations in Fixed and Fluidized Bed Apparatuses, Khimia, Leningrad, 1968
[31] Willhite, G. P., Kunii, D., Smith, J. M., Heat Transfer in Beds of Fine Particles (Heat Transfer Perpendicular to Flow), *AIChE J., 8* (1962), 3, pp. 340–345
[32] Li, C. H., Finlayson, B. A. , Heat Transfer in Packed Beds – A Reevaluation, *Chem. Eng. Sci., 32* (1977), pp. 1055–1066
[33] Beveridge, G. S. G., Haughey, D. P., Axial Heat Transfer in Packed Bed Beds. Stagnant Beds between 20 and 750 °C, *Int. J. Heat Mass Transfer, 14* (1971), pp. 1093–1113

[34] Hristov, J. Y., Fluidization of Ferromagnetic Particles in a Magnetic Field. Part 1: The Effect of the Field Lines Orientation on Bed Stability, *Powder Technology, 87* (1996), pp. 59–66
[35] Rosensweig, R. E., Fluidization: Hydrodynamics Stabilization with a Magnetic Field, *Science, 204* (1979), pp. 57–60
[36] Rosensweig, R. E., Siegel, J. H., Lee, W. K., Mikus, T., Magnetically Stabilized Fluidized Solids, *AIChE J.*, Symp. Ser., *77* (1981), 205, pp. 8–16
[37] Rosensweig, R. E., Process for Operating a Magnetically Stabilized Fluidized Bed, U. S. Patent 4 125 927, Sept. 24, 1980
[38] Hristov, J. Y., Fluidization of Ferromagnetic Particles in a Magnetic Field. Part 2: Field Effects of Preliminarily Fluidized Beds, *Powder Technology, 97* (1998), pp. 35–44
[39] Brich, M. A., Ganzha, V. L., Saxena, S. C., On the Design of Heat-Transfer Probes, *Int. Comm. Heat Mass Transfer, 24* (1997), pp. 151–159
[40] Kunii, D., Levenspiel, O., Fluidization Engineering, 2nd edn., Butterworth-Heinemann, Boston, 1991, pp. 1–13, pp. 69–75
[41] Kondratiev, G. M., Regular Heat Transfer Regime, M. GITTL, 1954, pp. 230–240
[42] Geiger, G. H.. Porier, D. R., Transport Phenomena in Metallurgy, Addison-Wesley, Reading, 1973, pp. 298–300
[43] Penchev, I. P., Hristov, J. Y., Behaviour of Fluidized Beds of Ferromagnetic Particles in an Axial Magnetic Field, *Powder Technology, 61* (1990), pp. 103–118
[44] Penchev, I. P., Hristov, J. Y., Fluidization of Ferromagnetic Particles in a Transverse Magnetic Field, *Powder Technology, 62* (1990), pp. 1–11
[45] Geldart, D., Types of Gas Fluidization, *Powder Technology, 7* (1973), pp. 285–292
[46] Kunii, D., Levenspiel, O., Fluidization Engineering, 2nd edn., Butterworth-Heinemann, Boston, 1991, pp. 1–13, pp, 69–75
[47] Jovanović, N. G., Colakyan, P., Jovanić, P., Vuković, D. V., Performance of Magnetically Stabilized Fluidized Beds, 8th Congress CHISA 84, paper No 767, Prague, Czech Republic, Sept. 3–7, 1984
[48] Jovanović, Z. R., Jovanović, G. N.,Vinjak-Novaković, G., Effect of Magnetic Field on Bubble Behaviour in Partially Stabilized Gas-Ferromagnetic Particles Fluidized Beds., *Proceedings.* 2nd Yugoslavian Chemical and Process Engineering, May 11–15, Dubrovnik, v. *2.* (1987), pp. 30–34
[49] Ganzha, V. L., Upadyay, S. N., Saxena, S. C., A Mechanistic Theory for the Heat Transfer between Fluidized Beds of Large Particles and Immersed Surfaces, *Int.J. Heat Mass Transfer, 25* (1982), pp. 1531–1540
[50] Ganzha, V. L., Heat and Mass Transfer in Dispersed Media with Two-Phase Flow., D. Sc. Thesis, Luikov Inst. Heat Mass Transfer (ITMO), Minsk, Belarus, 1992
[51] Saxena, S. C., Ganzha, V. L., Heat Transfer to Immersed Surfaces in Gas-Fluidized Beds of Large Particles and Powder Classification, *Powder Technology, 39* (1984), pp. 199–208
[52] Krasnostchekov, E. A., Sukomel, A. S., Manual on Heat Transfer, 4th ed., Energia, Moscow, 1980

Author's address:

Jordan Y. Hristov
Department of Chemical Engineering
University of Chemical Technology and Metallurgy
1756 Sofia, 8 Kl. Ochridsky str., Bulgaria
E-mail: jyh@uctm.edu

Paper submited: January 10, 2000
Paper revised: March 15, 2000
Paper accepted: April 5, 2000